Sex- and APOE ε4-dependent expression patterns of the Cannabinoid Receptor-1, FAAH, and MAGL are weakened in late-onset Alzheimer disease frontocortical samples

Ryan M. Heistad
University of Saskatchewan
Jennifer N.K. Nyarko
University of Saskatchewan
Paul R. Pennington
University of Saskatchewan
Huzaifa Saeed
University of Saskatchewan
Lais V.B. Gomes
University of Saskatchewan
Darrell D. Mousseau
darrell.mousseau@usask.ca

University of Saskatchewan

Research Article

Keywords: Alzheimer disease, endocannabinoid system, CB1R-60/-47/-37, sex-dependent, APOE ε4 risk allele, brain region, autopsy tissues

Posted Date: June 12th, 2026

DOI: https://doi.org/10.21203/rs.3.rs-9717404/v1

Additional Declarations: No competing interests reported.

Sex- and *APOE* ε4-dependent expression patterns of the Cannabinoid Receptor-1, FAAH, and MAGL are weakened in late-onset Alzheimer disease frontocortical samples.

Ryan M. Heistad[1], Jennifer N.K. Nyarko[1], Paul R. Pennington[1], Huzaifa Saeed[1,2], Lais V.B. Gomes[1], and Darrell D. Mousseau[1,*]

1: Cell Signalling Laboratory, Department of Psychiatry, College of Medicine, University of Saskatchewan, Saskatoon, SK, Canada.
2: Current address - Department of Anesthesiology, Perioperative Medicine, and Pain Management, College of Medicine, University of Saskatchewan, Saskatoon, SK, Canada.

*: correspondence: D.D. Mousseau, Cell Signalling Laboratory, University of Saskatchewan, GD30.6 HSB, 107 Wiggins Rd., Saskatoon, SK (S7N 5E5), Canada.
Tel: (306) 966-8824; e-mail: darrell.mousseau@usask.ca

Running title: The ECS is altered in the late-onset AD brain (37/46)

Abstract:

Background: The expression levels of the Cannabinoid Receptor-1 (CB1R) and enzymes of endocannabinoid metabolism, *e.g.* FAAH and MAGL, are rarely compared concurrently in Alzheimer disease (AD) brain tissue and often rely on mRNA transcript levels, which may not always reflect the expression levels of the corresponding proteins.

Methods: Western blotting was used to examine the expression levels of CB1R, FAAH, and MAGL proteins in autopsy cortical and corresponding hippocampal samples obtained from neurologically normal controls and donors with a diagnosis of either early-onset AD (<65 yrs) or late-onset AD (>65 yrs). The study included male and female donors.

Results: Our examination revealed several CB1R immunoreactive bands, and the mean expression levels of CB1Rs, FAAH, or MAGL were mostly consistent between control, EOAD, and LOAD samples. Linear regression revealed (predominantly cortical) associations amongst the CB1R species as well as between CB1Rs and either FAAH or MAGL when data were stratified by sex alone. Unexpectedly, stratifying by *APOE* ε4 status (independent of diagnosis) revealed strong associations in male non-carriers of the ε4 risk allele as well as in female carriers of the ε4 allele. When stratified by 'diagnosis', associations were evident in control and EOAD samples but were far less frequent in LOAD samples.

Conclusions: Our observations suggest that fundamental sex-/*APOE* ε4-dependent regulation of the cortical Endocannabinoid System may be negatively impacted during the protracted course of the late-onset form of AD. It remains to be determined whether such a deficit underpins neuropsychiatric or neurodegenerative phenotypes associated with the disease course.

Key words: Alzheimer disease; endocannabinoid system; CB1R-60/-47/-37; sex-dependent; *APOE* ε4 risk allele; brain region; autopsy tissues

Introduction.

The endocannabinoid system (ECS) distributes throughout the brain [1] and has been implicated in brain health and neurotransmission [2] as well as in processes that underpin mood and neuropsychiatric phenotypes [3] and degenerative diseases and therapies [4,5]. The ECS involves two cannabinoid receptors (CB1R, CB2R). The CB1R is ubiquitously expressed in brain, whereas the CB2R is expressed at far lower levels and may have more (sub)regional or cell type-specific (and inducible) distribution [6]. This report will focus on the CB1R.

The endogenous ECS ligands are N-arachidonoyl-ethanolamine (anandamide: AEA) [7] and 2-arachidonoyl glycerol (2-AG) [8] and a gas chromatography/mass spectrometry study of rapidly frozen rat brain estimated 2-AG levels to be 174 times greater than those of AEA [9]. Fatty acid amide hydrolase (FAAH) and monoacylglycerol lipase (MAGL) are the primary enzymes responsible for AEA [10] and 2-AG [11] degradation, respectively. As estimating brain levels of AEA and 2-AG can be challenging [9,12], the expression levels of FAAH and MAGL are sometimes used as proxies for the abundance of AEA and 2-AG.

ECS ligands are synthesized post-synaptically and act as retrograde neuromodulators [13]. Super-resolution microscopy confirms the localization of the CB1R to the presynaptic terminal, yet there is also evidence of expression of the CB1R on glia, with implied roles in brain, neurotransmitter homeostasis, and synaptogenesis already attributed to this cell type [14]. The distribution of MAGL and the CB1R to pre-synaptic terminals may allow MAGL to inactivate 2-AG within proximity of its site of action, whereas the distribution of FAAH to post-synaptic terminals may allow regulation of AEA availability close to its site of synthesis [15-17]. This disparate distribution of enzymes and sites of ligand inactivation are now thought to provide distinct roles for the two ligands, with 2-AG acting as a retrograde neuromodulator and AEA underpinning tonic actions of the ECS and

contributing to synaptic plasticity, potentially in a region-dependent manner [18,19]. The influence of ECS ligands *via* the CB1R on several neurotransmitter systems, notably GABA and glutamate [20], and their modulation of transmitter release that indirectly affects long-term potentiation and depression [21], aligns well with the role of the ECS in memory and cognition [4]. Additional interactions with monoaminergic systems [22] implicate the ECS in mood and neuropsychiatric disorders [23-25]. Preclinical (animal) models often align with clinical evidence and support a role for the ECS in, for example, post-traumatic stress disorder [26], stress resilience [27], nausea and vomiting [28] as well as in anxiety, schizophrenia and depression [29-31].

There is strong interest in defining the influence of the ECS during the course of diseases of the brain associated with aging, such as Alzheimer disease (AD) (see reviews [4,32-34]). AD presents with behavioral and cognitive deficits that reflect pathology centered on the hippocampus and associated structures [35], which appear to spread from pathology that is triggered across different cortical regions; such a phenomenon is associated with normal aging, but exacerbated in AD [36]. Interestingly, CB1R densities are relatively higher in these two regions [37]. Aside from advancing age [38], other risk factors, such as biological sex [39] and genetics [40], including the *APOE* ε4 risk allele [41], are helping to identify modifiable events within the earlier stages of AD progression. The majority of cases of AD present clinically after 65 years of age and these late-onset cases of AD (LOAD) are of unknown cause, although markers of the disease can be identified 20+ years before onset of symptoms, *e.g.* [42]. Cases of early-onset AD (EOAD) account for fewer than 10% of all cases of AD and are distinguished as non-mendelian (non-familial) cases (~8%) or the rare, genetic cases that involve mutations in the *APP*, *PSEN1* or *PSEN2* genes (~1-2%) that tend to increase levels of toxic β-amyloid (Aβ) length variants [43,44]. The response of the CB1R in AD remains somewhat ambiguous, with losses in density (*e.g.* [45,46]) and no differences from age-matched

controls (*e.g.* [47,48]) being reported. FAAH and MAGL also may exert different effects during different stages of AD/dementia [49], which would alter endogenous ligand availability and CB1R number and functionality [50,51].

We chose to examine components of the ECS ―CB1R, FAAH, and MAGL― in human autopsy brain samples from neurologically normal controls and cases of EOAD and LOAD. We observed sporadic differences between the mean expression of any one of the proteins, regardless of stratification of data (*e.g.* by sex or by *APOE* ε4 status or by diagnosis). In contrast, linear regression revealed associations between these components in cortical samples if data were stratified by basic characteristics, *e.g.* by sex or by *APOE* ε4 status. Many of these associations were maintained in control and EOAD samples but were far weaker or absent in LOAD samples when the stratification focused on 'diagnosis'. In addition, we observed far fewer associations in the corresponding hippocampal samples. Our observations may be reflecting the heterogeneity of the disease itself [52-54] or may be reflecting region-dependent pathological patterns, *e.g.* [55]. The fact that associations are observed in control and EOAD samples but are not as evident in LOAD samples suggests *a priori* that disruption of the ECS is not generalizable to all cases of 'AD'. Rather, a loss of regulation or adaptability of the ECS may ensue over the protracted course of the later onset cases of the disease, which would, in turn, suggest different ECS-based pharmacotherapeutic strategies may benefit cases of EOAD *vs*. LOAD. We are currently investigating whether levels of CB1R, FAAH, or MAGL align with either Aβ or Tau pathology or with neurochemical changes in these same human tissue sets.

Experimental procedures.

Human brain samples. Autopsied cortical samples were obtained from the Douglas–Bell Canada

Brain Bank (McGill University, Montréal, Canada) under the University of Saskatchewan's Research Ethics Office Certificate of Approval: Bio 06-124 (DDM: Principal Investigator). Sixty male and female (M/F) samples include 26 controls (12M/14F), 16 EOAD (*i.e.*, age of onset <65 years: 7M/9F), and 18 LOAD (*i.e.*, age of onset >65 years: 8M/10F) (see **Table 1**). Their information includes Age-at-Onset (AAO: presentation of symptoms), duration (in years), and *APOE* ε4 status (based on restriction isotyping [*e.g.*, rs429358 (APOE-C112R) and rs7412 (APOE-R158C)] as reported previously [56]). None of these cases of EOAD are carriers of any of the mutations in *PSEN1*, *PSEN2*, or *APP* genes that have been linked to the rare autosomal dominant forms of EOAD [57], suggesting they are cases of non-mendelian EOAD [43]. All cases of AD were confirmed neuropathologically at intake according to the CERAD criteria. Cortical samples corresponding to a mix of superior and middle frontal cortices (BA9/46, respectively) were chosen as they are associated with executive function and cognition, and relative hypoperfusion in AD patients [58]. Regional variation between components of the ECS was explored by comparing these cortical samples with corresponding hippocampal samples from the same donors. Our hippocampal AD samples, *e.g.* EOAD (7M/8F), and LOAD (8M/10F), were well matched in number, although several of the control hippocampal samples were not available (depleted at source) and we recognize this as a possible limitation of the study.

CNR1 (cannabinoid receptor 1) transcript expression using semi-quantitative PCR. Total RNA was isolated from pestle-homogenized brain tissue (50-100 mg) using the RNeasy® Plus Universal Mini Kit (Qiagen; cat#: 73404). RNA (1 μg: quantified using nano-drop spectrophotometry) was reverse-transcribed using the iScript Select cDNA Synthesis Kit (Bio-Rad; cat# 170-8897) and cDNA was quantified by nanodrop spectrophotometry. Transcripts of interest were amplified by

standard polymerase chain reaction (PCR) using 500 ng of the respective cDNA and Platinum Taq DNA Polymerase (Invitrogen; cat#10966-034). The Forward (F) and Reverse (R) primer pairs for the coding sequence were based on GenBank sequence (accession# BC100968.1) as reported elsewhere [59], whereas the primer pair spanning Exon1-Exon4 were designed based on human *CNR1*, transcript variant 1, NCBI (NM_016083.4). The primer pairs were: (a) *CNR1* (amplicon = 165 bp): (F) 5'-AAG GTG ACA TGG CAT CCA AAT and (R) 5'-AGG ACG AGA GAG ACT TGT TGT AA; (b) *CNR1* Spanning Intron (amplicon = 265 bp): (F) (in Exon 1) 5'-AGG ACC AGG GGA TGC GAA GG and (R) (in Exon 4) 5'-AAT TTG GAT GCC ATG TCA CCT T; (c) Succinate dehydrogenase (SDH: used as internal control [60]; amplicon = 141 bp) (F) 5'-TCT GCC CAC ACC AGC ACT and (R) 5'-CCT CTC CAC GAC ATC CTT CC. Thermocycling relied on a denaturing step at 95°C (10 minutes), followed by 50 cycles of 95°C/58°C/72°C (10 seconds at each temperature), with a final extension at 72°C for 5 minutes. 10 μL of the reaction mixture was then resolved on a 2% agarose gel containing 5 μL/100mL GelRed Stain (Cat# 41003-Biotium) and run at 80V for 1 Hr (100 mL gel) in 0.5X TBE. Amplicons were visualized under UV light and quantified by densitometry (ImageJ 1.32j: http://rsb.info.nih.gov/ij/).

Antibodies and immunodetection. The anti-CB1R (cat#C1108) and anti-FAAH (WH0002166M7) antibodies were obtained from Sigma-Aldrich Ltd, while the anti-MAGL antibody (Ab24701) was obtained from Abcam Inc. The anti-GAPDH antibody (#14C10) was obtained from Cell Signaling Technologies. LICOR goat anti-rabbit or anti-mouse secondary antibodies [IRDye 800CW Goat anti-rabbit IgG (P/N 926-32211), IRDye 680RD Goat anti-rabbit IgG (P/N 926-68071), or IRDye 680RD Goat anti-mouse IgG (P/N 926-68070)] were obtained from Bio-Rad Laboratories (Canada) Ltd.

The RIPA buffer contained 50 mM Tris (pH7.5), 150 mM NaCl, 1% Nonidet P-40 (NP-40), 0.5% Sodium Deoxycholate, 1 mM EDTA, 0.1% SDS and freshly added cOmplete™, EDTA-free Protease Inhibitor Cocktail (Sigma-Aldrich Ltd, 4693132001).

Immunodetection conditions were first optimized using different denaturing temperatures and combinations of milk casein and/or BSA blocking buffers or buffers for incubation with the primary antibodies. In our hands, the signal-to-noise was far better when using BSA as a blocking agent.

Tissue samples (~30 mg) were disrupted in 20 volumes of RIPA using a pestle-homogenizer system and then passed five times through a 22-gauge needle. Samples were allowed to sit on ice for 30 minutes and then precleared by centrifugation (12,000×*g*, 10 min, 4 °C) and used for protein determination (Sigma Total Protein Kit: cat#TP0300). Samples were diluted in Laemmli Buffer to 1 μg/μl and heated for five minutes at 65°C (the lower temperature still denatures proteins, but avoids aggregation of glycosylated proteins, *e.g.* the CB1R): [61]). This assay was performed by a single individual so as to decrease inter-sampling variability.

Sample aliquots (25 μg protein/lane) were resolved by SDS-PAGE and then transferred to nitrocellulose membranes (230 mA, 90 minutes) and blocked with 1% BSA in TBST (TBS +0.2% Triton X-100) for 30 minutes. Membranes were then washed in TBST (3x10 minutes) and probed overnight at 4°C with primary antibody [anti-CB1R at 1:500; anti-FAAH at 1:1000; anti-MAGL at 1:1000] in 5% BSA TBST with 0.05% Tween20. Membranes were then washed in TBST (3x10 minutes) and incubated with secondary antibody (1:20,000 in 5% milk/TBST) for one hour at room temperature. Following three washes in TBST, membranes were scanned on an Odyssey Imager (LI-COR Biosciences). The expression of GAPDH was used to normalize protein expression levels.

Statistical analyses. Variability between group means was analyzed using either the Mann-Whitney U test or ANOVA ($\alpha = 0.05$) with *post hoc* multiple comparisons based on the Tukey test. In addition to comparing sample means based on diagnosis, *e.g.* control, EOAD, LOAD, we also examined the data based on stratification into homogeneous subgroups independent of diagnosis, *e.g.* by sex alone or by *APOE* ε4 status. Simple linear regression was used to estimate any association between test variables. These analyses provided a *P* value ($P < 0.05$ set as significance) as well as R^2 (the coefficient of determination). All of the statistical analyses used in this report, even those results highlighted in graphical format, are supplied as *Supplementary Tables* (see **Supp Tables 1-28**). Any significant effects are discussed in the text. Note that our random sample set allowed us to analyze the data by diagnosis alone, sex alone, *APOE* ε4 status alone (carrier or not of the ε4 risk allele), sex-by-diagnosis, or sex-by-*APOE* ε4 status. Unfortunately, it did not allow us to stratify the data based on diagnosis-by-sex-by-*APOE* ε4 status, *e.g*. these random samples included a single *APOE* ε4(+) female control sample and a single *APOE* ε4(-) male LOAD sample (see **Table 1**; donor statistics).

Results.

CNR1 transcripts in human cortical extracts. Semi-quantitative PCR was used to estimate mRNA transcript levels of *CNR1* (the gene encoding the CB1R) in human brain (**Figure 1**). Two sets of primer-pairs led to distinct patterns. Transcript levels of succinate dehydrogenase (SDH, *e.g.* Complex II) were used to normalize amplicon intensity. A primer-pair within *CNR1* Exon 4, which contains the CB1R protein coding region and is the primary exon expressed in brain [62], revealed a fairly consistent pattern of expression across samples and no observable differences between

samples means whether stratified by diagnosis, by *APOE* ε4 status, or by sex alone (**Figure 1B-D**). In these same samples, we investigated the pattern of expression based on a primer-pair covering Exon 1 and Exon 4. We chose to examine this combination as Exon 1 contains multiple transcription starting sites [63] that may contribute to alternative *CNR1* transcription and CB1R function [64]. Exon 1-4 amplicons were not observed in some samples (suggesting a lack of Exon 1 transcription), whereas other samples produced slightly different amplicon sizes (**Figure 1A**).

Western blot analysis of components of the ECS in human brain.

Comparing data based on group means. We chose to use Western blotting to investigate the expression of the CB1R protein in our human autopsy sample set and observed three anti-CB1R immunoreactive bands (**Figure 2A**). Based on published reports, the 47-kDa form likely represents the immature CB1R (*e.g.*, with no post-translational modifications), whereas the 60-kDa form may represent a glycosylated (putatively active) form [65]. We also detected a triplet that migrated at approximately 37-kDa band; this band grouping has been described elsewhere as likely representing a putative splice variant rather than any degradation fragment(s) [66]. Aside from an increase in the 60-kDa CB1R band (CB1R-60) in the hippocampus of our EOAD and LOAD samples [P = 0.0065] (**Figure 2B**), we did not observe any changes in the mean expression of any of these CB1R bands between controls and either EOAD or LOAD samples (**Figure 2B-D**).

FAAH was detected as an expected ~60 kDa immunoreactive band [67] (**Figure 2A**) and although MAGL is detected as a 33/36 kDa doublet in the periphery, our immunoblots revealed MAGL migrates at or above 35 kDa (with a very minor band at ~37 kDa) in our patient samples, thus corroborating reports based on human brain and the U-87 MG (human glioblastoma-astrocytoma) cell line [68]. ANOVA did not reveal any overt changes in mean expression levels of

either cortical or hippocampal FAAH (**Figure 2E**) or MAGL (**Figure 2F**), regardless of diagnosis. This lack of central tendencies based on group means reflects the reports of inconsistent changes in the ECS in AD tissues [4]. We chose to use linear regression to question whether any variability around the means could be indicating associations in the expression of the different components of the ECS.

Using linear regression to determine whether associations exist between the components of the ECS in human brain.

We began by investigating whether basic characteristics such as age and sex of the donor exerted any influence on CB1R, FAAH, or MAGL expression, and then investigated factors such as the donor's diagnosis or genotype (*APOE* ε4 status; a risk factor for AD). Our analyses included 'pooled data', *e.g.* the pooling of male and female data, as well as data clustered by sex. The directionality of any significant association should be interpreted as 'positive', unless stated otherwise.

Alignment of ECS proteins with donor age.

We did not observe any association between the age of the donor and either cortical or hippocampal expression of CB1Rs (**SUPPL Table 1**) or FAAH or MAGL (**SUPPL Table 2**).

Alignment of ECS proteins with Age-at-Onset (AAO) of symptoms) or with duration of disease.

We observed negative associations between AAO *vs* cortical CB1R-47 in male EOAD (**SUPPL Table 3**) and AAO *vs* hippocampal CB1R-47 in pooled EOAD (**SUPPL Table 4**). There also were positive associations between AAO and cortical MAGL in pooled EOAD samples

(**SUPPL Table 5**) as well as between AAO and both hippocampal FAAH and MAGL (**SUPPL Table 5**) in pooled EOAD samples. Disease duration associated with male cortical CB1R-60 and CB1R-47 in EOAD samples (**SUPPL Table 6**) as well as with pooled hippocampal CB1R-60, which was driven primarily by males (**SUPPL Table 7**). Neither FAAH nor MAGL (regardless of region) associated with duration (**SUPPL Table 8**).

Alignment of ECS proteins based on data stratified by sex alone. We did not observe any change in mean expression of CB1R-60, CB1R-47, or CB1R-37 based solely on the donor's sex in either our cortical samples (**Figure 3A-C**) or the corresponding hippocampal samples (**SUPPL Figure 1**). Linear regression revealed associations in both sexes between CB1R-60 and CB1R-47 (**Figure 3D**) and between CB1R-60 and CB1R-37 (**Figure 3E**; **SUPPL Table 9**). There was only an association between CB1R-47 and CB1R-37 in females (**Figure 3F**). We did not observe any association of any of the CB1R species in the hippocampus (**SUPPL Table 9**). Mean FAAH levels were lower in female cortical [P = 0.0092] (**Figure 4A**) and hippocampal [P = 0.0249] samples (**Figure 4D**), whereas MAGL levels were similar between the sexes in both regions (**Figure 4B, 4E).** Linear regression revealed an association between FAAH and MAGL levels in both male and female cortical samples (**Figure 4C**) as well as in female hippocampal samples (**Figure 4E**). There was no alignment of either FAAH or MAGL levels between regions (**SUPPL Table 10**).

Levels of FAAH were associated with levels of both CB1R-60 (**Figure 5A**) and CB1R-47 (**Figure 5B**) in both male and female cortical samples but only aligned with levels of CB1R-37 in female cortical samples (**Figure 5C**; **SUPPL Table 11**). Levels of MAGL also aligned with levels of the CB1Rs in female cortical samples (**Figure 5D-F**) but only aligned with male CB1R-47 levels (**Figure 5E**; **SUPPL Table 11**). Aside from an association between hippocampal MAGL

and CB1R-47 in male samples, there were no other significant associations between either FAAH or MAGL and CB1Rs in this region (**SUPPL Table 11**).

These associations observed solely on the sex of the donor support an inherent role of brain FAAH and/or MAGL (and presumed endogenous ligand availability) in the regulation of CB1R levels. We next investigated whether any of these observed associations were impacted by a diagnosis of AD, whether it be EOAD or LOAD.

Alignment of ECS proteins based on data stratified by diagnosis. Our regression analyses –when data were stratified for diagnosis– revealed associations between the expression of CB1R species were confined to pooled (male and female) control and EOAD samples, with a significant influence by female donors (**Table 2**). There were no associations between the expression of the various CB1R species in LOAD samples, aside from an association between CB1R-47 and CB1R-37 in male samples (**Table 2**). Only sporadic associations were observed in the hippocampal samples (**SUPPL Table 12**). When comparing CB1R expression levels between regions, we only observed association between cortical and hippocampal CB1R-60 (male and female) and between cortical and hippocampal CB1R-37 (female) EOAD samples (**SUPPL Table 13**).

Alignment of FAAH and MAGL within regions based on data stratified by diagnosis. We observed associations between FAAH and MAGL levels within male and female cortical (**Figure 6**) and hippocampal (**Figure 7**) control samples. Any associations in EOAD and LOAD samples aligned with one sex or the other, but not both (**Figures 6-7**; **Table 3**). We observed an inter-regional association between FAAH levels but not for MAGL levels (**Table 3**).

Alignment of either FAAH or MAGL and CB1Rs within regions based on data stratified by diagnosis. Linear regression revealed associations between cortical FAAH and CB1R-60 as well as CB1R-47 in control male samples and between FAAH and CB1R-47 in female EOAD and LOAD samples (**SUPPL Table 14**). Hippocampal samples only revealed an association between FAAH and CB1R-47 in female control samples (**SUPPL Table 15**). In contrast, we observed associations between MAGL and both CB1R-47 and CB1R-37 in CTL, EOAD, and LOAD cortical samples (**Figure 8**; **SUPPL Table 16**) and between MAGL and CB1R-47 in CTL, EOAD, and LOAD hippocampal samples with diagnosis-specific contributions by males or females (**SUPPL Table 17**).

The lack of any generalized patterns of association between CB1Rs and FAAH or MAGL based on a diagnosis of EOAD or LOAD could be reflecting the complex nature of disease progression in the AD brain or with the diagnosis of AD itself [69,70]. The *APOE* ε4 allele is known to exert different levels of risk in males and females [41] and a donor's *APOE* ε4 status is simple, *e.g.* either they carry the allele or they do not. Recently, our own reports suggested that phenotypes often associated with AD such as Aβ levels [56,71] or some of the depression-related proteins implicated in AD-related risk [72,73] often present with a stronger phenotype if data are stratified simply by *APOE* ε4 status rather than by the donor's diagnosis. With this in mind, we investigated whether any changes in the ECS could align simply with the donor's *APOE* ε4 status.

Alignment of different CB1R bands within regions based on data stratified by APOE ε4 status. We first compared group means when CB1R data were stratified simply by the donor's *APOE* ε4 status (*e.g.* carrier of the ε4 risk allele or not). Except for a significant increase in CB1R-60 expression in hippocampal samples of carriers of the ε4 allele [P = 0.0276] (**SUPPL Figure 2**),

with contributions from both male [P = 0.0456] and female [p = 0.0344] carriers (**SUPPL Figure 3**), the expression levels of CB1Rs based on *APOE* ε4 status were unchanged in our cortical and hippocampal samples.

Regression analysis of pooled data revealed associations between CB1R-60 and CB1R-47 (**Figure 9A**), between CB1R-60 and CBR1-37 (**Figure 9D**), and between CB1R-47 and CB1R-37 (**Figure 9G**) in carriers as well as in non-carriers of the ε4 allele. Clustering the *APOE* ε4 stratification by sex revealed that these associations were all evident in female samples, regardless of *APOE* ε4 status, whereas in males only the CB1R-60/CB1R-47 and CB1R-47/CB1R-37 associations were significant and only observed in carriers of the allele (**Figure 9B, C, E, F, H, I**; **SUPPL Table 18**). In the hippocampal tissues, aside from a few instances, *e.g.* CB1R-60/CB1R-47 [pooled ε4 carriers] and CB1R-60/CB1R-37 in male non-carriers (**SUPPL Table 19**), we did not observe any other significant associations.

Alignment of FAAH and MAGL within regions based on data stratified by APOE ε4 status. *APOE* ε4 status did not reveal any difference between carriers and non-carriers in either cortical or hippocampal mean FAAH levels (**SUPPL Figure 4A, C**) or mean MAGL levels (**SUPPL Figure 4B, D**).

Regression analysis revealed associations between FAAH and MAGL expression levels in cortical samples in non-carriers of the allele as well as in female carriers of the allele (**Figure 10A-C**). In hippocampal samples, associations between FAAH and MAGL expression levels were evident in male non-carriers and in female carriers of the allele (**Figure 10D-F**) (and **SUPPL Table 20**). We did not observe any associations between cortical and hippocampal FAAH (or MAGL) levels (**SUPPL Table 20**).

Alignment of CB1Rs and either FAAH or MAGL based on data stratified by APOE ε4 status.

Cortical FAAH expression associated with CB1Rs in females (regardless of their ε4 status) (**Figure 11**), whereas any association between FAAH and CB1Rs (specifically CB1R-60 and CB1R-47) were only observed in male non-carriers (**Figure 11B, E**; **SUPPL Table 21**). We did not observe any associations between FAAH expression and CB1Rs in the corresponding hippocampal samples (**SUPPL Table 22**). Similarly, we observed associations between MAGL and CB1R-60, -47, and -37 in cortical female samples regardless of *APOE* ε4 status (**Figure 12**; **SUPPL Table 23**). However, the only associations in males were observed between MAGL and CB1R-47 in non-carriers (**Figure 12E**) and between MAGL and CB1R-37 in carriers (**Figure 12I**). In the hippocampus, we observed an association between MAGL and CB1R-60 in female non-carriers and between MAGL and CB1R-47 in male carriers of the allele (**SUPPL Table 24**).

We re-visited the AAO and duration of disease when the dataset was stratified simply by *APOE* ε4 status (*i.e.* independent of 'diagnosis') and observed that cortical CB1R-60 and CB1R-47 levels were negatively associated with AAO, but only in male carriers of the ε4 allele (**SUPPL Table 25**). Interestingly, CB1R-60 and CB1R-47 expression was associated with a longer duration of disease in these same ε4-positive males (**SUPPL Table 26**). These associations were not evident in the hippocampal data (**SUPPL Tables 27-28**).

Discussion.

Most cases (>90%) of AD are diagnosed following a protracted disease course with pathological triggers potentially preceding clinical symptoms by 20+ years [42]. Components of the ECS, whether it be the CB1R or one of the enzymes (*e.g.* FAAH or MAGL) that are involved in regulating levels of the endocannabinoids, have been implicated in AD and their potential as

pharmacotherapeutic targets is discussed in numerous reviews on the topic [32,34,74-76].

We did not observe any change in *CNR1* mRNA expression in AD samples and opted to examine the expression of the CB1R protein itself. Quantification of CB1R expression and function often rely on ligand-receptor or GTPγS binding assays, or on immunohistochemical detection. These approaches have provided valuable information on CB1R function and/or distribution, but invariably assume a single CB1R entity. In fact, the literature acknowledges multiple anti-CB1R immunodetectable bands, three of which guided our labeling of the bands we observed by Western blot. These include a ~60-kDa band that may represent a post-translationally modified CB1R (*e.g.*, glycosylation with heterogeneous carbohydrate composition; based on studies in rat [65]) and a ~47-kDa band that migrates at the expected molecular weight of the deduced amino acid sequence for the protein-coding sequence of the *CNR1* transcript (*e.g.*, without any post-translational modifications) [65]. A ~37-kDa band is proposed to be a putative splice variant and while bands at ~50 and ~35 kDa have been reported to co-express in the same brain tissues [77], they may partition to different synaptic compartments, suggesting different functions [66]. *CNR1* splice variants have been shown to have a higher affinity for 2-AG (*vs.* AEA), which appears to act as an inverse agonist on these variants (based on GTPγS activity) [78]. These variants may play a role in neuropsychiatric diseases such as schizophrenia, bipolar disorder, and major depression [64], all of which present with cognitive deficits. The presence of multiple bands in our samples adds to the interpretation of CB1R expression during AD. For example, glycosylation of CB1R may not alter its ligand-binding affinity, but it does increase its stability and expression at the cell membrane [79], which is critical for regulating the receptor's functionality [80,81]. The only change we observed in the mean relative expression levels of any of the CB1R species was an increase in this putatively glycosylated CB1R-60 in EOAD and LOAD hippocampal samples (that may be

influenced by the donor's *APOE* ε4 status; *see* **SUPPL Fig. 4**). This would align with reports that activation of the CB1R in hippocampus alters GABA availability and hinders long-term potentiation, thereby impairing synaptic strength and memory consolidation (reviewed in [82]). The general absence of change in mean expression of CB1R or FAAH or MAGL in our AD sample set was intriguing, but does reflect other reports on the variability in ECS marker expression in AD samples (reviewed in [4,32,34,74-76]). In addition, our analyses did not reveal any generalizable differences in mean expression of these three proteins based strictly on the donor's sex or *APOE* ε4 status (in either brain region). This lack of change is interesting given that we have observed, based on these same autopsy samples, pathology-relevant changes in mean relative expression of markers of other systems, several of which were clearly dependent on sex or *APOE* ε4 status of the donor and altered in both EOAD and LOAD samples; these include markers of the serotonin synapse [72], the mitochondrial enzymes monoamine oxidases A and B [73], and, of course, markers of AD-related amyloid pathology, including the Aβ peptide and related secretases [56,71].

Whereas mean relative expression levels of these components of the ECS did not reveal any striking patterns, regression analysis revealed unique information. Associations between CB1Rs, FAAH, or MAGL expression levels were evident primarily in cortical samples and were evident even if data were simply stratified by *APOE* ε4 status or sex alone; this suggests that co-dependent regulation of the ECS is an inherent character of the system within the cortex. Several of these associations were less frequent in LOAD samples but were maintained in control as well as in EOAD samples (*recall*, these are non-genetic cases of AD). The loss of associations in LOAD samples was not a function of age of the donor but could be reflecting distinct underlying pathologies between EOAD and LOAD, or a compensatory mechanism that loses its capacity to adapt over the longer course of LOAD (*e.g.* 20+ years [42]). For example, we observed associations

between FAAH and MAGL in control, EOAD, and LOAD samples, which would suggest that any disease-related deficit in connectivity would affect both pre- and post-synaptic membranes equally. We also observed associations between MAGL and either CB1R-47 or CB1R-37 that were maintained, to some degree, in LOAD samples; however, the few associations between FAAH and CB1Rs were limited to control and EOAD samples. *A priori*, this would suggest that MAGL (*vs.* FAAH) has more influence on CB1R regulation in these brain samples. The fact that expression levels of CB1R(-47/-37) align with MAGL (which hydrolyzes almost 85% of the brain's 2-AG [83]) suggests that 2-AG availability may be significantly impacted in AD. This assumption is derived from the fundamental principles of receptor regulation: *e.g.* an increase in MAGL would lead to increase degradation of 2-AG. In turn, the loss of 2-AG would lead to CB1R upregulation. Thus, a positive association between MAGL and CB1Rs would imply a loss of 2-AG. The fact that we do not observe a complete loss of associations between CB1Rs and MAGL in LOAD samples may be reflecting the report that, during the course of AD, MAGL expression may not change but a pool of MAGL may be recruited to an 'improper' localization within the cell, thereby affecting 2-AG termination and signaling [47]. Thus, levels of the MAGL protein may not necessarily align with changes in its functionality and its influence on CB1R expression in the AD brain. Pathway effects of FAAH and MAGL inhibitors suggest roles for FAAH in stress paradigms and roles for MAGL in inflammation in relation to health and disease, with opposing effects of AEA and 2-AG on decision-making and cognitive flexibility (reviewed in [84]). Again, the improper localization of MAGL within the cell during the course of AD may alter 2-AG termination and signaling [47] and CB1R function. Our observations may also be indirectly confirming that our LOAD samples may represent a heterogenous disease that it is far more complex than a simple diagnostic label, *e.g.* AD, would assume [70]. Indeed, LOAD is now thought

to represent several types and subtypes as confirmed by CSF proteomics [52], RNA seq [53], and visual rating scales of brain atrophy [54]. Furthermore, autoradiography studies of post-mortem AD tissues using selective CB1R radioligands [^{3}H]CP55,940 [85] and [^{125}I]SD-7015 [86] have already suggested CB1R density may undergo a bi-phasic response during the disease course, with an increase in early Braak staging and then diminishing as Tau pathology is exacerbated, and may follow a subregion-specific response (*e.g.*, within cortical layers or within hippocampal subfields). A similar loss of CB1R based on Braak staging was observed in a recent immunohistochemical study of AD brain regions [87]. The *hAPP*/*PSEN1*(△Ex9) mouse [88] and the 3xTg-AD mouse [89] also suggest a loss of CB1R density is associated with progression of pathology. The mouse strain may also hold some critical information in these studies as it was shown that CB1R expression was reduced in 5- and 9-month old 5xFAD mouse cortex, but only in the 9-month old 5xFAD hippocampus, whereas expression of the CB1R was not reduced in the Tg4-42 mouse cortex, but was reduced in the corresponding hippocampus [87]. An ongoing investigation in our laboratory based on the 'J20' [Tg(PDGFB-*APPSwInd*)] mouse has revealed associations between expression levels of the various CB1Rs limited to hippocampal samples, whereas associations between CB1Rs and both FAAH and MAGL, observed primarily in the cortex, are actually enhanced by the $hAPP_{Swe/Ind}$ transgene (RMH and DDM, *unpublished data*). The fact our observations in J20 mice appear to differ from phenotypes observed in 3xTg-AD [89], 5xFAD [87,90], or APP_{Swe}/PS1ΔE9 [91] mice, all of which also carry some familial AD-related variant of the *PSEN1* gene, is intriguing and may be implicating the presenilin-1-sensitive, opposing influences of 2-AG and AEA on Notch signaling [92].

Any reports of an influence of *APOE* ε4 status on the ECS enzymes centers on FAAH in stroke [93] and atherosclerosis [94] and MAGL in CB2R-sensitive atherosclerosis [95]. It is well known that sex

[96] and the *APOE* ε4 allele can influence risk of LOAD and amyloid burden (particularly in females) [41,56], and that ECS targeting and therapeutic response in AD/dementia can be complicated by influences of sex [97] and *APOE* ε4 status [98,99]. It is surprising, therefore, that there is a paucity of data regarding the influence of these two risk factors on ECS proteins in the same AD tissues.

Our analyses revealed several associations between these components of the ECS in samples from both sexes but also revealed several associations that were predominantly found in female donors. The role of the CB1R in brain is complicated as it would appear that males may have significantly higher CB1R density [100], while CB1R density in females may increase over the lifespan [101]. Of course, this is further complicated by region-dependent patterns and sex-dependent regional vulnerabilities; for example, female 5xFAD mice exhibit earlier prefrontocortical lesions progressing to hippocampus-related deficits in later stages, whereas male 5xFAD mice show damage mainly in the hippocampus [102]. An immunohistochemical study did not find any significant difference in expression levels of CB1R across *APOE* genotypes [87], whereas a PET study did not find any difference in CB1R density between AD patients and cognitively intact controls, regardless of *APOE* ε4 status [48]; unfortunately, male and female data were pooled in both cases and the potential for sex-specific trends was not addressed. The few reports of an influence of *APOE* ε4 status on the ECS in AD/dementia centers on cognitive phenotypes in older individuals with metabolic syndrome [99] or dampening of any beneficial effect of exercise on memory in young carriers of the risk allele [98]. We observed changes in CB1R expression that tended to align with an earlier age-at-onset of symptoms in male carriers of the *APOE* ε4 allele, yet these same males lived longer with their symptoms. This may indirectly be corroborating the increased risk of AD associated with the ε4 allele in women, but not men [41]. A recent study found that male carriers of the *APOE* ε4 allele with a clinical diagnosis of depression were far more at

risk for dementia in later life than males without a history of depression [103]. Unfortunately, that study focused exclusively on males and it is unclear if the same trend holds true for females with depression. Somewhat counterintuitively, testosterone provides far more relief of cognitive deficits in female mice carrying the *APOE* ε4 allele [104]. The fact that we observe a similar association between CB1Rs and AAO or duration limited to male EOAD, but not LOAD, samples (when stratified by diagnosis) argues further for sex-dependent adaptive responses of the ECS that tend to be negatively impacted during the longer disease course associated with the later onset form of the disease.

2-AG concentrations have also been reported to be negatively correlated with baseline cognition and cognitive changes in men and carriers of the *APOE* ε4 allele, while in women, cognitive changes correlated with the abundance of AEA [99]. Interestingly, we found expression levels of CB1Rs associate with FAAH in both sexes but associate predominantly with MAGL in females and this is particularly evident when the data are stratified by *APOE* ε4 status or sex alone. At this time, we cannot explain the molecular events that would underpin similar associations between components of the ECS based on diametrically opposed sex-by-*APOE* ε4 groupings; for example, associations between FAAH and MAGL were evident in male non-carriers and in female carriers of the ε4 allele (**Figure 10D-F** and **SUPPL Table 20**). These observations are intriguing nonetheless and speak to clearly distinct fundamental ECS mechanisms in the male and female brain.

To the best of our knowledge, this is the first comparison of CB1R, FAAH, and MAGL expression levels in the same human brain tissues. A recent immunohistochemical study [105] examined the simultaneous distribution of these three key components of the ECS in pig claustrum and confirmed their peri-synaptic localization; MAGL tended to be presynaptic and also associated

with GFAP-positive cells (glia), whereas FAAH was localized to the post-synapse as well as parvalbumin-positive (Ca^{2+}-releasing) cells that are likely inhibitory interneurons (GABAergic) with a critical role in long-term depression. These observations corroborated studies that had examined various combinations of these components of the ECS in dogs, monkey, and rodents [105]. Our current study has revealed patterns of expression of these three ECS proteins that differ between human brain regions; that differ based on a diagnosis of EOAD *versus* LOAD; and that differ by sex and *APOE* ε4 status (with strong patterns in male non-carriers of the ε4 allele and in female carriers of the ε4 allele). While this report remains observational and cross-sectional, it does support distinct roles for the brain ECS across stages (or types) of AD or between the sexes. Given that several of the associations differ between EOAD and LOAD samples, we will investigate whether these changes in CB1R, FAAH, or MAGL align with either Aβ or Tau pathology in these same tissues. In addition, we recently reported that cannabinoids may be better suited to provide relief from behavioral and psychological symptoms, rather than cognitive deficits within the disease course [106]. As such, we will also investigate how the expression of these components of the ECS align with changes in monoaminergic tone in these same tissues [72].

Limitations.

We acknowledge that 2-AG and AEA interact with proteins other than the CB1R, *e.g.* [107,108], any one of which could also be contributing to AD-related phenotypes. A statistical limitation of this study and the interpretation of our data is that our random 60-sample set was not sufficiently powered to undertake relevant three-way stratification, i.e. sex-by-*APOE* ε4-by-diagnosis, although being able to compare between two brain regions from the same donor is an added value to our measured outcomes. Furthermore, we feel there is validity in our observations as we are still

able to observe associations in control and EOAD samples, but not LOAD samples, when the data are stratified by 'diagnosis' (even though sample sizes in all three groupings are smaller than in other stratifications).

It is known that the CB1R exerts different influences on synaptic function depending on its localization (*e.g.* primarily pre-synaptic, but also evidence of post-synaptic) and on which cell type it is expressed (glia, GABA-ergic, glutamatergic) [109]. Thus, we acknowledge that in the absence of subcellular fractionation of our brain samples, it is unclear which one of our immunodetectable CB1R bands could be contributing to the disease course and whether differences in cell type or in subcellular localization could be underpinning some of the differences we observe in the human brain. While a meta-analysis found little to no benefit of cannabinoids in AD [110], our own systematic review suggests that cannabinoids may be better suited to provide relief from behavioral and psychological symptoms of dementia, without any overt effect on cognitive phenotypes [106]. In the absence of any information on medication history or cannabinoid usage in the donor casefile, it is impossible to determine how much of the variability in the current study may be attributed to recreational or clinical cannabinoid usage. Finally, additional studies will need to determine whether our current observations are generalizable across other pathologies with a cognitive phenotype in which the ECS has been implicated, for example, Parkinson's disease [111], depression [112], or ALS [113], and in corresponding *in vivo* models.

Author contributions

RMH, JNN, and DDM: experimental design. RMH, JNN, PRP, HS, LVBG, and DDM: data collection and analysis. All authors were involved in editing the manuscript.

Acknowledgments

Parts of this work were presented at the 41st Annual Meeting of the Canadian College of Neuropsychopharmacology.

Funding

This work was funded, in part, by the Saskatchewan Research Chair (held by DDM) in *Alzheimer Disease and Related Dementia*, which is funded jointly by the Alzheimer Society of Saskatchewan and the Saskatchewan Health Research Foundation. DDM is also grateful to a local philanthropic donor for funding support.

Competing interests

The authors declare that there are no competing interests.

References.

1. Mechoulam R, Parker LA. The endocannabinoid system and the brain. *Annu Rev Psychol.* 2013;64:21-47.
2. Kano M, Ohno-Shosaku T, Hashimotodani Y, Uchigashima M, Watanabe M. Endocannabinoid-mediated control of synaptic transmission. *Physiol Rev.* 2009;89(1):309-380.
3. Micale V, Di Marzo V, Sulcova A, Wotjak CT, Drago F. Endocannabinoid system and mood disorders: priming a target for new therapies. *Pharmacol Ther.* 2013;138(1):18-37.
4. Basavarajappa BS, Shivakumar M, Joshi V, Subbanna S. Endocannabinoid system in neurodegenerative disorders. *J Neurochem.* 2017;142(5):624-648.
5. Paes-Colli Y, Aguiar AFL, Isaac AR, et al. Phytocannabinoids and Cannabis-Based Products as Alternative Pharmacotherapy in Neurodegenerative Diseases: From Hypothesis to Clinical Practice. *Front Cell Neurosci.* 2022;16:917164.
6. Chen DJ, Gao M, Gao FF, Su QX, Wu J. Brain cannabinoid receptor 2: expression, function and modulation. *Acta Pharmacol Sin.* 2017;38(3):312-316.
7. Devane WA, Axelrod J. Enzymatic synthesis of anandamide, an endogenous ligand for the cannabinoid receptor, by brain membranes. *Proc Natl Acad Sci U S A.* 1994;91(14):6698-6701.
8. Sugiura T, Kishimoto S, Oka S, Gokoh M. Biochemistry, pharmacology and physiology of 2-arachidonoylglycerol, an endogenous cannabinoid receptor ligand. *Prog Lipid Res.* 2006;45(5):405-446.
9. Stella N, Schweitzer P, Piomelli D. A second endogenous cannabinoid that modulates long-term potentiation. *Nature.* 1997;388(6644):773-778.
10. Deutsch DG, Chin SA. Enzymatic synthesis and degradation of anandamide, a cannabinoid receptor agonist. *Biochem Pharmacol.* 1993;46(5):791-796.
11. Goparaju SK, Ueda N, Yamaguchi H, Yamamoto S. Anandamide amidohydrolase reacting with 2-arachidonoylglycerol, another cannabinoid receptor ligand. *FEBS Lett.* 1998;422(1):69-73.
12. Brose SA, Golovko SA, Golovko MY. Brain 2-Arachidonoylglycerol Levels Are Dramatically and Rapidly Increased Under Acute Ischemia-Injury Which Is Prevented by Microwave Irradiation. *Lipids.* 2016;51(4):487-495.
13. Kreitzer AC, Regehr WG. Retrograde signaling by endocannabinoids. *Curr Opin Neurobiol.* 2002;12(3):324-330.
14. Bernal-Chico A, Tepavcevic V, Manterola A, Utrilla C, Matute C, Mato S. Endocannabinoid signaling in brain diseases: Emerging relevance of glial cells. *Glia.* 2023;71(1):103-126.
15. Katona I, Sperlagh B, Sik A, et al. Presynaptically located CB1 cannabinoid receptors regulate GABA release from axon terminals of specific hippocampal interneurons. *J Neurosci.* 1999;19(11):4544-4558.
16. Yoshida T, Uchigashima M, Yamasaki M, et al. Unique inhibitory synapse with particularly rich endocannabinoid signaling machinery on pyramidal neurons in basal amygdaloid nucleus. *Proc Natl Acad Sci U S A.* 2011;108(7):3059-3064.
17. Gulyas AI, Cravatt BF, Bracey MH, et al. Segregation of two endocannabinoid-hydrolyzing enzymes into pre- and postsynaptic compartments in the rat hippocampus, cerebellum and amygdala. *Eur J Neurosci.* 2004;20(2):441-458.

18. Kim J, Alger BE. Reduction in endocannabinoid tone is a homeostatic mechanism for specific inhibitory synapses. *Nat Neurosci.* 2010;13(5):592-600.
19. Bisogno T, Berrendero F, Ambrosino G, et al. Brain regional distribution of endocannabinoids: implications for their biosynthesis and biological function. *Biochem Biophys Res Commun.* 1999;256(2):377-380.
20. Howlett AC, Barth F, Bonner TI, et al. International Union of Pharmacology. XXVII. Classification of cannabinoid receptors. *Pharmacol Rev.* 2002;54(2):161-202.
21. Misner DL, Sullivan JM. Mechanism of cannabinoid effects on long-term potentiation and depression in hippocampal CA1 neurons. *J Neurosci.* 1999;19(16):6795-6805.
22. Ashton CH, Moore PB. Endocannabinoid system dysfunction in mood and related disorders. *Acta Psychiatr Scand.* 2011;124(4):250-261.
23. Hill MN, Gorzalka BB. Is there a role for the endocannabinoid system in the etiology and treatment of melancholic depression? *Behav Pharmacol.* 2005;16(5-6):333-352.
24. Carvalho AF, Van Bockstaele EJ. Cannabinoid modulation of noradrenergic circuits: implications for psychiatric disorders. *Prog Neuropsychopharmacol Biol Psychiatry.* 2012;38(1):59-67.
25. Garani R, Watts JJ, Mizrahi R. Endocannabinoid system in psychotic and mood disorders, a review of human studies. *Prog Neuropsychopharmacol Biol Psychiatry.* 2021;106:110096.
26. Mayo LM, Rabinak CA, Hill MN, Heilig M. Targeting the Endocannabinoid System in the Treatment of Posttraumatic Stress Disorder: A Promising Case of Preclinical-Clinical Translation? *Biol Psychiatry.* 2022;91(3):262-272.
27. Dudek KA, Paton SEJ, Binder LB, et al. Astrocytic cannabinoid receptor 1 promotes resilience by dampening stress-induced blood-brain barrier alterations. *Nat Neurosci.* 2025;28(4):766-782.
28. DeVuono MV, Venkatesan T, Hillard CJ. Endocannabinoid signaling in stress, nausea, and vomiting. *Neurogastroenterol Motil.* 2025;37(3):e14911.
29. Patel S, Hillard CJ. Role of endocannabinoid signaling in anxiety and depression. *Curr Top Behav Neurosci.* 2009;1:347-371.
30. Rodriguez-Munoz M, Sanchez-Blazquez P, Callado LF, Meana JJ, Garzon-Nino J. Schizophrenia and depression, two poles of endocannabinoid system deregulation. *Transl Psychiatry.* 2017;7(12):1291.
31. Shen B, Wang Z, Yu H, et al. Medicinal cannabis oil improves anxiety-like and depressive-like behaviors in CCS mice via the BDNF/TRPC6 signaling pathway. *Behav Brain Res.* 2024;467:115005.
32. Uddin MS, Mamun AA, Sumsuzzman DM, et al. Emerging Promise of Cannabinoids for the Management of Pain and Associated Neuropathological Alterations in Alzheimer's Disease. *Front Pharmacol.* 2020;11:1097.
33. Chen C. Endocannabinoid metabolism and Alzheimer's disease. *Neural Regen Res.* 2022;17(9):1987-1988.
34. Li S, Huang Y, Yu L, Ji X, Wu J. Impact of the Cannabinoid System in Alzheimer's Disease. *Curr Neuropharmacol.* 2023;21(3):715-726.
35. West MJ. Regionally specific loss of neurons in the aging human hippocampus. *Neurobiol Aging.* 1993;14(4):287-293.

36. Giannakopoulos P, Hof PR, Michel JP, Guimon J, Bouras C. Cerebral cortex pathology in aging and Alzheimer's disease: a quantitative survey of large hospital-based geriatric and psychiatric cohorts. *Brain Res Brain Res Rev.* 1997;25(2):217-245.
37. Herkenham M, Lynn AB, Little MD, et al. Cannabinoid receptor localization in brain. *Proc Natl Acad Sci U S A.* 1990;87(5):1932-1936.
38. Richard E, Schmand B, Eikelenboom P, Westendorp RG, Van Gool WA. The Alzheimer myth and biomarker research in dementia. *J Alzheimers Dis.* 2012;31(0):S203-209.
39. Brady B, Zheng L, Kootar S, Anstey KJ. Sex and gender differences in risk scores for dementia and Alzheimer's disease among cisgender, transgender, and non-binary adults. *Alzheimers Dement.* 2024;20(1):5-15.
40. Bekris LM, Galloway NM, Millard S, et al. Amyloid precursor protein (APP) processing genes and cerebrospinal fluid APP cleavage product levels in Alzheimer's disease. *Neurobiol Aging.* 2011;32(3):556 e513-523.
41. Poirier J, Davignon J, Bouthillier D, Kogan S, Bertrand P, Gauthier S. Apolipoprotein E polymorphism and Alzheimer's disease. *Lancet.* 1993;342(8873):697-699.
42. Villemagne VL, Burnham S, Bourgeat P, et al. Amyloid beta deposition, neurodegeneration, and cognitive decline in sporadic Alzheimer's disease: a prospective cohort study. *Lancet Neurol.* 2013;12(4):357-367.
43. Reitz C, Rogaeva E, Beecham GW. Late-onset vs nonmendelian early-onset Alzheimer disease: A distinction without a difference? *Neurol Genet.* 2020;6(5):e512.
44. Sirkis DW, Bonham LW, Johnson TP, La Joie R, Yokoyama JS. Dissecting the clinical heterogeneity of early-onset Alzheimer's disease. *Mol Psychiatry.* 2022;27(6):2674-2688.
45. Ramirez BG, Blazquez C, Gomez del Pulgar T, Guzman M, de Ceballos ML. Prevention of Alzheimer's disease pathology by cannabinoids: neuroprotection mediated by blockade of microglial activation. *J Neurosci.* 2005;25(8):1904-1913.
46. Solas M, Francis PT, Franco R, Ramirez MJ. CB2 receptor and amyloid pathology in frontal cortex of Alzheimer's disease patients. *Neurobiol Aging.* 2013;34(3):805-808.
47. Mulder J, Zilberter M, Pasquare SJ, et al. Molecular reorganization of endocannabinoid signalling in Alzheimer's disease. *Brain.* 2011;134(Pt 4):1041-1060.
48. Ahmad R, Goffin K, Van den Stock J, et al. In vivo type 1 cannabinoid receptor availability in Alzheimer's disease. *Eur Neuropsychopharmacol.* 2014;24(2):242-250.
49. Aso E, Andres-Benito P, Ferrer I. Delineating the Efficacy of a Cannabis-Based Medicine at Advanced Stages of Dementia in a Murine Model. *J Alzheimers Dis.* 2016;54(3):903-912.
50. Chanda PK, Gao Y, Mark L, et al. Monoacylglycerol lipase activity is a critical modulator of the tone and integrity of the endocannabinoid system. *Mol Pharmacol.* 2010;78(6):996-1003.
51. Zhong P, Pan B, Gao XP, Blankman JL, Cravatt BF, Liu QS. Genetic deletion of monoacylglycerol lipase alters endocannabinoid-mediated retrograde synaptic depression in the cerebellum. *J Physiol.* 2011;589(Pt 20):4847-4855.
52. Tijms BM, Gobom J, Reus L, et al. Pathophysiological subtypes of Alzheimer's disease based on cerebrospinal fluid proteomics. *Brain.* 2020;143(12):3776-3792.
53. Neff RA, Wang M, Vatansever S, et al. Molecular subtyping of Alzheimer's disease using RNA sequencing data reveals novel mechanisms and targets. *Sci Adv.* 2021;7(2).

54. Ferreira D, Verhagen C, Hernandez-Cabrera JA, et al. Distinct subtypes of Alzheimer's disease based on patterns of brain atrophy: longitudinal trajectories and clinical applications. *Sci Rep.* 2017;7:46263.
55. Byun MS, Kim SE, Park J, et al. Heterogeneity of Regional Brain Atrophy Patterns Associated with Distinct Progression Rates in Alzheimer's Disease. *PLoS One.* 2015;10(11):e0142756.
56. Nyarko JNK, Quartey MO, Pennington PR, et al. Profiles of beta-Amyloid Peptides and Key Secretases in Brain Autopsy Samples Differ with Sex and APOE epsilon4 Status: Impact for Risk and Progression of Alzheimer Disease. *Neuroscience.* 2018;373:20-36.
57. Campion D, Dumanchin C, Hannequin D, et al. Early-onset autosomal dominant Alzheimer disease: prevalence, genetic heterogeneity, and mutation spectrum. *Am J Hum Genet.* 1999;65(3):664-670.
58. Levy-Cooperman N, Burhan AM, Rafi-Tari S, et al. Frontal lobe hypoperfusion and depressive symptoms in Alzheimer disease. *J Psychiatry Neurosci.* 2008;33(3):218-226.
59. Ludanyi A, Eross L, Czirjak S, et al. Downregulation of the CB1 cannabinoid receptor and related molecular elements of the endocannabinoid system in epileptic human hippocampus. *J Neurosci.* 2008;28(12):2976-2990.
60. Larrinaga G, Sanz B, Perez I, et al. Cannabinoid CB(1) receptor is downregulated in clear cell renal cell carcinoma. *J Histochem Cytochem.* 2010;58(12):1129-1134.
61. Smith RD, Baukal AJ, Zolyomi A, et al. Agonist-induced phosphorylation of the endogenous AT1 angiotensin receptor in bovine adrenal glomerulosa cells. *Mol Endocrinol.* 1998;12(5):634-644.
62. Zhang PW, Ishiguro H, Ohtsuki T, et al. Human cannabinoid receptor 1: 5' exons, candidate regulatory regions, polymorphisms, haplotypes and association with polysubstance abuse. *Mol Psychiatry.* 2004;9(10):916-931.
63. Shire D, Calandra B, Delpech M, et al. Structural features of the central cannabinoid CB1 receptor involved in the binding of the specific CB1 antagonist SR 141716A. *J Biol Chem.* 1996;271(12):6941-6946.
64. Tao R, Li C, Jaffe AE, et al. Cannabinoid receptor CNR1 expression and DNA methylation in human prefrontal cortex, hippocampus and caudate in brain development and schizophrenia. *Transl Psychiatry.* 2020;10(1):158.
65. Song C, Howlett AC. Rat brain cannabinoid receptors are N-linked glycosylated proteins. *Life Sci.* 1995;56(23-24):1983-1989.
66. Saumell-Esnaola M, Barrondo S, Garcia Del Cano G, et al. Subsynaptic Distribution, Lipid Raft Targeting and G Protein-Dependent Signalling of the Type 1 Cannabinoid Receptor in Synaptosomes from the Mouse Hippocampus and Frontal Cortex. *Molecules.* 2021;26(22).
67. Giang DK, Cravatt BF. Molecular characterization of human and mouse fatty acid amide hydrolases. *Proc Natl Acad Sci U S A.* 1997;94(6):2238-2242.
68. van der Vliet D, Klinkenberg AXY, Platte R, et al. Spatially Resolved Mapping of Monoacylglycerol Lipase Activity in the Brain. *ACS Chem Neurosci.* 2025;16(24):4622-4635.
69. Kamatham PT, Shukla R, Khatri DK, Vora LK. Pathogenesis, diagnostics, and therapeutics for Alzheimer's disease: Breaking the memory barrier. *Ageing Res Rev.* 2024;101:102481.

70. Jack CR, Jr., Andrews JS, Beach TG, et al. Revised criteria for diagnosis and staging of Alzheimer's disease: Alzheimer's Association Workgroup. *Alzheimers Dement.* 2024;20(8):5143-5169.
71. Quartey MO, Nyarko JNK, Maley JM, et al. The Abeta(1-38) peptide is a negative regulator of the Abeta(1-42) peptide implicated in Alzheimer disease progression. *Sci Rep.* 2021;11(1):431.
72. Nyarko JNK, Quartey MO, Heistad RM, et al. Glycosylation States of Pre- and Post-synaptic Markers of 5-HT Neurons Differ With Sex and 5-HTTLPR Genotype in Cortical Autopsy Samples. *Front Neurosci.* 2018;12:545.
73. Quartey MO, Nyarko JNK, Pennington PR, et al. Alzheimer Disease and Selected Risk Factors Disrupt a Co-regulation of Monoamine Oxidase-A/B in the Hippocampus, but Not in the Cortex. *Front Neurosci.* 2018;12:419.
74. Xiong Y, Lim CS. Understanding the Modulatory Effects of Cannabidiol on Alzheimer's Disease. *Brain Sci.* 2021;11(9).
75. Abate G, Uberti D, Tambaro S. Potential and Limits of Cannabinoids in Alzheimer's Disease Therapy. *Biology (Basel).* 2021;10(6).
76. Ferreira PCL, Bellaver B, Povala G, et al. Endocannabinoid System Biomarkers in Alzheimer's Disease. *Cannabis Cannabinoid Res.* 2023;8(1):77-91.
77. Bagher AM, Laprairie RB, Kelly ME, Denovan-Wright EM. Co-expression of the human cannabinoid receptor coding region splice variants (hCB(1)) affects the function of hCB(1) receptor complexes. *Eur J Pharmacol.* 2013;721(1-3):341-354.
78. Ryberg E, Vu HK, Larsson N, et al. Identification and characterisation of a novel splice variant of the human CB1 receptor. *FEBS Lett.* 2005;579(1):259-264.
79. Rapino C, Castellucci A, Lizzi AR, et al. Modulation of Endocannabinoid-Binding Receptors in Human Neuroblastoma Cells by Tunicamycin. *Molecules.* 2019;24(7).
80. Lutz B. Neurobiology of cannabinoid receptor signaling. *Dialogues Clin Neurosci.* 2020;22(3):207-222.
81. Fletcher-Jones A, Hildick KL, Evans AJ, Nakamura Y, Henley JM, Wilkinson KA. Protein Interactors and Trafficking Pathways That Regulate the Cannabinoid Type 1 Receptor (CB1R). *Front Mol Neurosci.* 2020;13:108.
82. Figueiredo A, Cheer JF. Endocannabinoid regulation of hippocampus-dependent memory. *Exp Neurol.* 2023;364.
83. Blankman JL, Simon GM, Cravatt BF. A comprehensive profile of brain enzymes that hydrolyze the endocannabinoid 2-arachidonoylglycerol. *Chem Biol.* 2007;14(12):1347-1356.
84. Ren SY, Wang ZZ, Zhang Y, Chen NH. Potential application of endocannabinoid system agents in neuropsychiatric and neurodegenerative diseases-focusing on FAAH/MAGL inhibitors. *Acta Pharmacol Sin.* 2020;41(10):1263-1271.
85. Manuel I, Gonzalez de San Roman E, Giralt MT, Ferrer I, Rodriguez-Puertas R. Type-1 cannabinoid receptor activity during Alzheimer's disease progression. *J Alzheimers Dis.* 2014;42(3):761-766.
86. Farkas S, Nagy K, Palkovits M, et al. [(1)(2)(5)I]SD-7015 reveals fine modalities of CB(1) cannabinoid receptor density in the prefrontal cortex during progression of Alzheimer's disease. *Neurochem Int.* 2012;60(3):286-291.

87. von Borke N, Purwien AV, Steiert A, Hasecke H, Bouter Y. Reduced CB1 Cannabinoid Receptor Expression in Alzheimer's Disease and Transgenic Mouse Models. *Aging Medicine.* 2026;0:1-17.
88. Kalifa S, Polston EK, Allard JS, Manaye KF. Distribution patterns of cannabinoid CB1 receptors in the hippocampus of APPswe/PS1DeltaE9 double transgenic mice. *Brain Res.* 2011;1376:94-100.
89. Bedse G, Romano A, Cianci S, et al. Altered expression of the CB1 cannabinoid receptor in the triple transgenic mouse model of Alzheimer's disease. *J Alzheimers Dis.* 2014;40(3):701-712.
90. Vazquez C, Tolon RM, Grande MT, et al. Endocannabinoid regulation of amyloid-induced neuroinflammation. *Neurobiol Aging.* 2015;36(11):3008-3019.
91. Vidal-Palencia L, Ramon-Duaso C, Gonzalez-Parra JA, Busquets-Garcia A. Gene Expression Analysis of the Endocannabinoid System in Presymptomatic APP/PS1 Mice. *Front Pharmacol.* 2022;13:864591.
92. Frampton G, Coufal M, Li H, Ramirez J, DeMorrow S. Opposing actions of endocannabinoids on cholangiocarcinoma growth is via the differential activation of Notch signaling. *Exp Cell Res.* 2010;316(9):1465-1478.
93. Cramer SC, Parodi L, Moslemi Z, et al. Genetic Variation and Stroke Recovery: The STRONG Study. *Stroke.* 2024;55(8):2094-2102.
94. Hoyer FF, Khoury M, Slomka H, et al. Inhibition of endocannabinoid-degrading enzyme fatty acid amide hydrolase increases atherosclerotic plaque vulnerability in mice. *J Mol Cell Cardiol.* 2014;66:126-132.
95. Vujic N, Schlager S, Eichmann TO, et al. Monoglyceride lipase deficiency modulates endocannabinoid signaling and improves plaque stability in ApoE-knockout mice. *Atherosclerosis.* 2016;244:9-21.
96. Mielke MM. Sex and Gender Differences in Alzheimer's Disease Dementia. *Psychiatr Times.* 2018;35(11):14-17.
97. Matheson J, Behzad D, Zakala C, et al. Sex differences in the acute effects of cannabis on human cognition: A systematic review. *Front Neuroendocrinol.* 2025;79:101215.
98. Igloi K, Marin Bosch B, Kuenzi N, et al. Interactions between physical exercise, associative memory, and genetic risk for Alzheimer's disease. *Cereb Cortex.* 2024;34(5).
99. Soldevila-Domenech N, Fagundo B, Cuenca-Royo A, et al. Relationship between sex, APOE genotype, endocannabinoids and cognitive change in older adults with metabolic syndrome during a 3-year Mediterranean diet intervention. *Nutr J.* 2024;23(1):61.
100. Laurikainen H, Tuominen L, Tikka M, et al. Sex difference in brain CB1 receptor availability in man. *Neuroimage.* 2019;184:834-842.
101. Van Laere K, Goffin K, Casteels C, et al. Gender-dependent increases with healthy aging of the human cerebral cannabinoid-type 1 receptor binding using [¹⁸F]MK-9470 PET. *Neuroimage.* 2008;39(4):1533-1541.
102. Ganesh A, Choudhury W, Coutellier L. Early spatial recognition memory deficits in 5XFAD female mice are associated with disruption of prefrontal parvalbumin neurons. *Brain Research.* 2024;1841.
103. Irie F, Masaki KH, Petrovitch H, et al. Apolipoprotein E epsilon4 allele genotype and the effect of depressive symptoms on the risk of dementia in men: the Honolulu-Asia Aging Study. *Arch Gen Psychiatry.* 2008;65(8):906-912.

104. Raber J, Bongers G, LeFevour A, Buttini M, Mucke L. Androgens protect against apolipoprotein E4-induced cognitive deficits. *J Neurosci.* 2002;22(12):5204-5209.
105. Pirone A, Lazzarini G, Lenzi C, Giannessi E, Miragliotta V. Immunolocalization of cannabinoid receptor 1 (CB1), monoglyceride lipase (MGL) and fatty-acid amide hydrolase 1 (FAAH) in the pig claustrum. *J Chem Neuroanat.* 2020;109:101843.
106. Bahji A, Breward N, Duff W, et al. Cannabinoids in the management of behavioral, psychological, and motor symptoms of neurocognitive disorders: a mixed studies systematic review. *J Cannabis Res.* 2022;4(1):11.
107. Baggelaar MP, Maccarrone M, van der Stelt M. 2-Arachidonoylglycerol: A signaling lipid with manifold actions in the brain. *Prog Lipid Res.* 2018;71:1-17.
108. Muller C, Morales P, Reggio PH. Cannabinoid Ligands Targeting TRP Channels. *Front Mol Neurosci.* 2018;11:487.
109. Busquets-Garcia A, Bains J, Marsicano G. CB(1) Receptor Signaling in the Brain: Extracting Specificity from Ubiquity. *Neuropsychopharmacology.* 2018;43(1):4-20.
110. Bosnjak Kuharic D, Markovic D, Brkovic T, et al. Cannabinoids for the treatment of dementia. *Cochrane Database Syst Rev.* 2021;9(9):CD012820.
111. Urmeneta-Ortiz MF, Tejeda-Martinez AR, Gonzalez-Reynoso O, Flores-Soto ME. Potential Neuroprotective Effect of the Endocannabinoid System on Parkinson's Disease. *Parkinsons Dis.* 2024;2024:5519396.
112. Gallego-Landin I, Garcia-Baos A, Castro-Zavala A, Valverde O. Reviewing the Role of the Endocannabinoid System in the Pathophysiology of Depression. *Front Pharmacol.* 2021;12:762738.
113. Denton TT, Carter GT, Goddard M, et al. Amyotrophic Lateral Sclerosis, the Endocannabinoid System, and Exogenous Cannabinoids: Current State and Clinical Implications. *Muscle Nerve.* 2025.

Figure legends

Figure 1. *CNR1* transcripts in human control and Alzheimer disease brain samples. (**A**) Amplicons generated by primer pairs within Exon 4 (Ex4) and spanning Exon1 and Exon4 of *CNR1* cDNA in neurologically normal control (CTL), early-onset AD (EO), and late-onset AD (LO) male (M) and female (F) samples. Levels of a succinate dehydrogenase (*SDH*) amplicon was used as an internal control. NTC (no template control) and cDNA (a plasmid construct containing the *CNR1* Exon4 cDNA) were used as negative and positive controls, respectively. The relative expression of *CNR1*(Ex4-Ex4) to *SDH* amplicons are expressed (**B**) by the donor's diagnosis, (**C**) by the donor's *APOE* ε4 status, *e.g.*, non-carriers: ε4(-); carriers: ε4(+), or (**D**) by the donor's sex alone.

Figure 2. Expression levels of markers of the ECS in human cortical and hippocampal samples stratified by diagnosis. (**A**) Representative immunoblots of Cannabinoid Receptor 1 (CB1R), FAAH, MAGL, and GAPDH (loading control) in human neurologically normal control (NC), early-onset AD (EO), and late-onset AD (LO) samples. The anti-CB1R antibody reveals CB1R immunodetetctable bands at ~60 kDa, ~47 kDa, and ~37 kDa. The levels (*y*-axis expressed as target protein/GAPDH) of (**B**) CB1R-60, (**C**) CB1R-47, (**D**) CB1R-37, (**E**) FAAH, and (**F**) MAGL in cortical (Cx) and hippocampal (Hippo) samples are presented by diagnosis. *: $P < 0.05$ between indicated groups. '{' indicates the three bands pooled for CB1R-37 kDa densitometry.

Figure 3. Expression levels of CB1Rs in cortical samples stratified by sex alone. The levels of (**A**) CB1R-60, (**B**) CB1R-47, and (**C**) CB1R-37 grouped according to the donor's sex [●: male; ○: female]. (**D-F**) The association (linear regression) between cortical (**D**) CB1R-60 and CB1R-47,

(**E**) CB1R-60 and CB1R-37, and (**F**) CB1R-47 and CB1R-37. Regression statistics (*e.g.* P value and R2) are indicated for each grouping and summarized in **SUPPL Table 9**. The dotted lines represent the 95% confidence interval for the slope of the respective regression lines.

Figure 4. Expression levels of FAAH and MAGL in cortical and hippocampal samples stratified by sex alone. The levels of (**A**) FAAH and (**B**) MAGL in cortical samples grouped according to the donor's sex [●: male; ○: female] and (**C**) the corresponding regression analysis between FAAH and MAGL. The levels of (**D**) FAAH and (**E**) MAGL and (**F**) regression analysis in corresponding hippocampal samples. *: $P < 0.05$ and **: $P < 0.01$ between indicated groups. Regression statistics (*e.g.* P value and R2) are indicated for each grouping and summarized in **SUPPL Table 10**. The dotted lines represent the 95% confidence interval for the slope of the respective regression lines.

Figure 5. Association between CB1Rs and either FAAH or MAGL levels in cortical samples stratified by sex alone. The association (linear regression) between FAAH and (**A**) CB1R-60, (**B**) CB1R-47, and (**C**) CB1R-37 and between MAGL and (**D**) CB1R-60, (**E**) CB1R-47, and (**F**) CB1R-37 are depicted. Regression statistics (*e.g.* P value and R2) are indicated for each grouping and summarized in **SUPPL Table 11**. The dotted lines represent the 95% confidence interval for the slope of the respective regression lines. ●: male; ○: female.

Figure 6. Association between FAAH and MAGL levels in cortical samples stratified by

diagnosis. The association (linear regression) between FAAH and MAGL in (**A**) neurologically normal control (●), (**B**) EOAD (▼), and (**C**) LOAD (▲) samples. (**D-F**) The same datasets separated by sex of the donor (filled symbols: male; open symbols: female). Regression statistics (*e.g.* P value and R2) are indicated for each grouping and summarized in **Table 3**. The dotted lines represent the 95% confidence interval for the slope of the respective regression lines.

Figure 7. Association between FAAH and MAGL levels in hippocampal samples stratified by diagnosis. The association (linear regression) between FAAH and MAGL in (**A**) neurologically normal control (●), (**B**) EOAD (▼), and (**C**) LOAD (▲) samples. (**D-F**) The same datasets separated by sex of the donor (filled symbols: male; open symbols: female). Regression statistics (*e.g.* P value and R2) are indicated for each grouping and summarized in **Table 3**. The dotted lines represent the 95% confidence interval for the slope of the respective regression lines.

Figure 8. Association between MAGL and CB1R-47 or CB1R-37 levels in cortical samples stratified by diagnosis. The association (linear regression) between MAGL in (**A**) CB1R-47 or (**B**) CB1R-37 in neurologically normal control (●), (**B**) EOAD (▼), and (**C**) LOAD (▲) samples. (**C-E**) The MAGL *vs* CB1R-47 dataset and (**F-I**) the MAGL *vs* CB1R-37 dataset separated by sex of the donor (filled symbols: male; open symbols: female). Regression statistics (*e.g.* P value and R2) are indicated for each grouping and summarized in **SUPPL Table 16**. The dotted lines represent the 95% confidence interval for the slope of the respective regression lines.

Figure 9. Association between the three CB1R species in cortical samples stratified by the donor's *APOE* ε4 status. The association (linear regression) between (**A**) CB1R-60 and CB1R-47, (**D**) CB1R-60 and CB1R-37, and (**G**) CB1R-47 and CB1R-37 in smaples startified by the donor's *APOE* ε4 status [*e.g.* [■: (-)ε4; non-carriers; □: (+)ε4: carriers]. The middle panels, e.g. **B, E, H**, depict non-carriers and panels at right, e.g. **C, F, I**, depict carirers of the ε4 allele clustered by sex of the donor (filled symbols: male; open symbols: female). Regression statistics (*e.g.* P value and R2) are indicated for each grouping and summarized in **SUPPL Table 18**. The dotted lines represent the 95% confidence interval for the slope of the respective regression lines.

Figure 10. Association between FAAH and MAGL levels in cortical samples stratified by by the donor's *APOE* ε4 status. The association (linear regression) between FAAH and MAGL in (**A**) cortical samples pooled by the donor's *APOE* ε4 status [*e.g.* [■: (-)ε4; non-carriers; □: (+)ε4: carriers]. Regression analysis of the cortical data clustered by the sex of (**B**) non-carriers and (**C**) carriers of the ε4 allele. (**D**) Regression analysis of corresponding pooled hippocampal data and the data clustered by the sex of (**B**) non-carriers and (**C**) carriers of the ε4 allele. Regression statistics (*e.g.* P value and R2) are indicated for each grouping and summarized in **SUPPL Table 20**. The dotted lines represent the 95% confidence interval for the slope of the respective regression lines.

Figure 11. Association between levels of FAAH and CB1Rs in cortical samples stratified by by the donor's *APOE* ε4 status. The association (linear regression) between FAAH and (**A**) CB1R-60, (**D**) CB1R-47, and (**G**) CB1R-37 in smaples startified by the donor's *APOE* ε4 status [*e.g.* [■:

(-)ε4; non-carriers; □: (+)ε4: carriers]. The middle panels, e.g. **B, E, H**, depict non-carriers and panels at right, e.g. **C, F, I**, depict carirers of the ε4 allele clustered by sex of the donor (filled symbols: male; open symbols: female). Regression statistics (*e.g.* P value and R2) are indicated for each grouping and summarized in **SUPPL Table 21**. The dotted lines represent the 95% confidence interval for the slope of the respective regression lines.

Figure 12. Association between levels of MAGL and CB1Rs in cortical samples stratified by by the donor's *APOE* ε4 status. The association (linear regression) between MAGL and (**A**) CB1R-60, (**D**) CB1R-47, and (**G**) CB1R-37 in smaples startified by the donor's *APOE* ε4 status [*e.g.* [■: (-)ε4; non-carriers; □: (+)ε4: carriers]. The middle panels, e.g. **B, E, H**, depict non-carriers and panels at right, e.g. **C, F, I**, depict carirers of the ε4 allele clustered by sex of the donor (filled symbols: male; open symbols: female). Regression statistics (*e.g.* P value and R2) are indicated for each grouping and summarized in **SUPPL Table 23**. The dotted lines represent the 95% confidence interval for the slope of the respective regression lines.

Control	N	Age (yrs: $\overline{x}$ ± std)	PMI (hrs: $\overline{x}$ ± std)	Onset (Age: $\overline{x}$ ± std)	Duration (yrs: $\overline{x}$ ± std)	*APOE* (-ε4/+ε4)
Pooled	26	70.73 ± 12.49	19.81 ± 12.36	—	—	21/5
Male	12	70.67 ± 9.85	16.43 ± 10.07	—	—	8/4
Female	14	70.79 ± 14.76	22.27 ± 13.72	—	—	13/1

EOAD	N	Age (yrs: $\overline{x}$ ± std)	PMI (hrs: $\overline{x}$ ± std)	Onset (Age: $\overline{x}$ ± std)	Duration (yrs: $\overline{x}$ ± std)	*APOE* (-ε4/+ε4)
Pooled	16	58.13 ± 7.80	19.73 ± 9.60	49.33 ± 7.92	9.20 ± 3.43	6/10
Male	7	63.14 ± 5.61	20.50 ± 10.24	56.50 ± 5.79	8.50 ± 3.94	3/4
Female	9	54.22 ± 7.16	19.30 ± 10.05	44.56 ± 4.95	9.67 ± 3.20	3/6

LOAD	N	Age (yrs: $\overline{x}$ ± std)	PMI (hrs: $\overline{x}$ ± std)	Onset (Age: $\overline{x}$ ± std)	Duration (yrs: $\overline{x}$ ± std)	*APOE* (-ε4/+ε4)
Pooled	18	83.17 ± 5.77	22.87 ± 6.45	74.44 ± 5.43	8.81 ± 3.41	3/15
Male	8	82.88 ± 5.38	25.21 ± 7.99	74.00 ± 4.55	8.14 ± 1.95	1/7
Female	10	83.40 ± 6.35	20.86 ± 4.45	74.78 ± 6.28	9.33 ± 4.27	2/8

Table 1: Summary of donor information, including neurologically normal, control donors and donors with a diagnosis of EOAD (Early-Onset AD) or LOAD (Late-Onset AD). De-identified information that was provided with the individual brain samples include the donor's sex, Age (years), PMI (post-mortem interval, hours), Age-At-Onset (presentation of symptoms), Duration of disease (does not apply to control donors), and *APOE* ε4 status (*e.g.* non-carriers (-ε4) or carriers (+ε4) of the risk allele). N: sample size; 'Pooled' = combined male and female data; 'yrs': years; 'hrs': hours

Cortex	60 *vs* 47	CTL		EOAD		LOAD	
		P = 0.0005↑		**P = 0.0473**↑		P = 0.0711	
		R^2 = 0.416		R^2 = 0.253		R^2 = 0.189	
	60 *vs* 47	Male	Female	Male	Female	Male	Female
		P = 0.1143	**P = 0.0086**↑	**P = 0.0033**↑	P = 0.3809	P = 0.1039	P = 0.3677
		R^2 = 0.230	R^2 = 0.481	R^2 = 0.847	R^2 = 0.111	R^2 = 0.380	R^2 = 0.102
Cortex	60 *vs* 37	CTL		EOAD		LOAD	
		P = 0.0004↑		P = 0.3573		P = 0.2031	
		R^2 = 0.425		R^2 = 0.061		R^2 = 0.099	
	60 *vs* 37	Male	Female	Male	Female	Male	Female
		P = 0.5462	**P = 0.0001**↑	P = 0.4852	P = 0.5455	P = 0.3759	P = 0.4901
		R^2 = 0.038	R^2 = 0.753	R^2 = 0.102	R^2 = 0.054	R^2 = 0.132	R^2 = 0.061
Cortex	47 *vs* 37	CTL		EOAD		LOAD	
		P < 0.0001↑		**P = 0.0232**↑		P = 0.0511	
		R^2 = 0.497		R^2 = 0.317		R^2 = 0.218	
	47 *vs* 37	Male	Female	Male	Female	Male	Female
		P = 0.5544	**P < 0.0001**↑	P = 0.1925	P = 0.1116	**P = 0.0169**↑	P = 0.4146
		R^2 = 0.036	R^2 = 0.884	R^2 = 0.312	R^2 = 0.321	R^2 = 0.641	R^2 = 0.085

Table 2: Linear regression by diagnosis – CB1R species *vs* CB1R species within cortex. CTL: control; EOAD: Early-Onset AD; LOAD: Late-Onset AD. Significant ($P \leq 0.05$) observations, if any, are identified in bold text. A positive association is identified by '↑'.

Within Cortex	FAAH vs MAGL	CTL		EOAD		LOAD	
		P < 0.0001↑		**P = 0.0080**↑		**P = 0.0034**↑	
		R^2 = 0.691		R^2 = 0.405		R^2 = 0.425	
	FAAH vs MAGL	Male	Female	Male	Female	Male	Female
		P = 0.0467↑	**P < 0.0001**↑	P = 0.8871	**P = 0.0045**↑	P = 0.0641	P = 0.3164
		R^2 = 0.340	R^2 = 0.835	R^2 = 0.004	R^2 = 0.708	R^2 = 0.461	R^2 = 0.125
Within Hippocampus	FAAH *vs* MAGL	CTL		EOAD		LOAD	
		P = 0.0033↑		**P = 0.0196**↑		P = 0.0783	
		R^2 = 0.427		R^2 = 0.353		R^2 = 0.205	
	FAAH vs MAGL	Male	Female	Male	Female	Male	Female
		P = 0.0086↑	**P = 0.0453**↑	**P = 0.0473**↑	P = 0.7576	P = 0.9351	**P = 0.0301**↑
		R^2 = 0.853	R^2 = 0.343	R^2 = 0.578	R^2 = 0.017	R^2 = 0.002	R^2 = 0.464
Cortex vs Hippocampus	FAAH *vs* FAAH	CTL		EOAD		LOAD	
		P = 0.0263↑		P = 0.3331		P = 0.1221	
		R^2 = 0.288		R^2 = 0.072		R^2 = 0.152	
	37 *vs* 37	Male	Female	Male	Female	Male	Female
		P = 0.4019	**P = 0.0386**↑	P = 0.9302	P = 0.4872	**P = 0.0232**↑	P = 0.9794
		R^2 = 0.180	R^2 = 0.394	R^2 = 0.002	R^2 = 0.084	R^2 = 0.676	R^2 = 0.000
Cortex vs Hippocampus	MAGL *vs* MAGL	CTL		EOAD		LOAD	
		P = 0.7802		P = 0.0549		P = 0.5351	
		R^2 = 0.005		R^2 = 0.255		R^2 = 0.028	
	MAGL *vs* MAGL	Male	Female	Male	Female	Male	Female
		P = 0.5371	P = 0.3027	P = 0.1411	P = 0.5084	P = 0.9406	P = 0.4523
		R^2 = 0.102	R^2 = 0.117	R^2 = 0.379	R^2 = 0.076	R^2 = 0.002	R^2 = 0.073

Table 3: Linear regression by diagnosis – FAAH and MAGL within and between cortex and hippocampus. CTL: control; EOAD: Early-Onset AD; LOAD: Late-Onset AD. Significant ($P \leq 0.05$) observations, if any, are identified in bold text. A positive association is identified by '↑'.

Figure 1: CNR1 transcripts in CTL and AD samples.

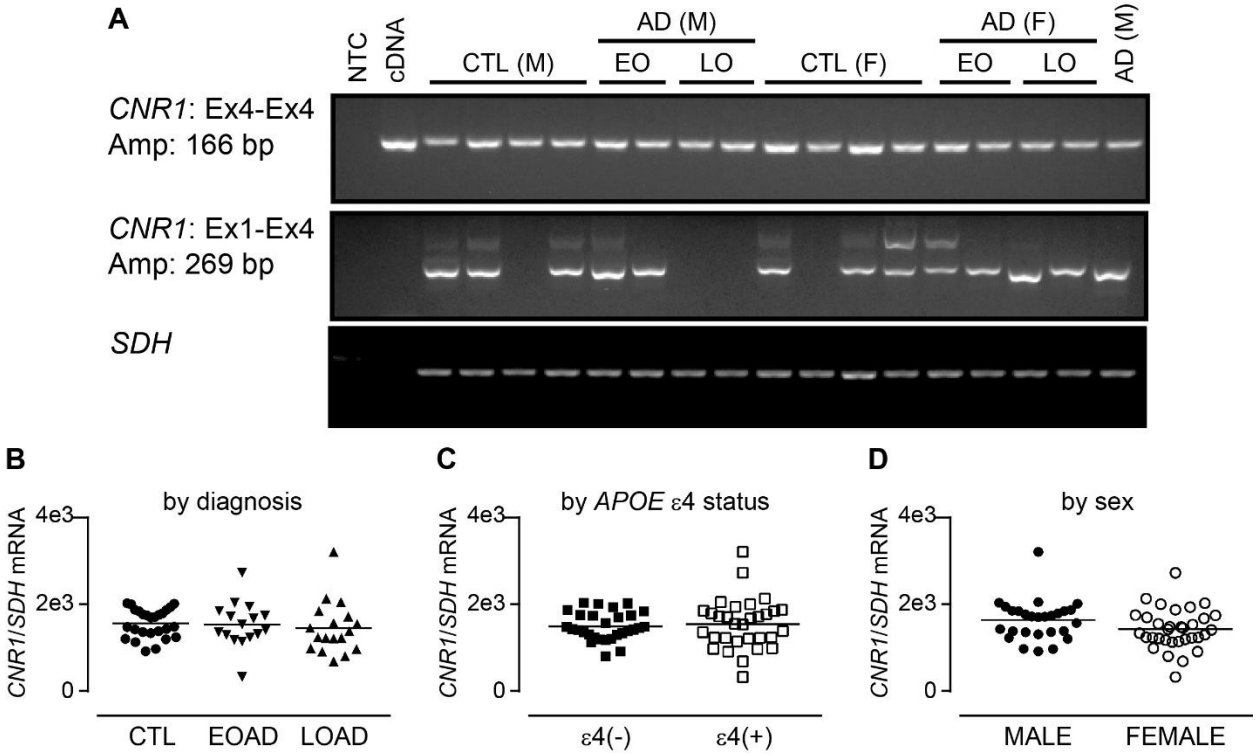

Figure 2: CB1Rs, FAAH, and MAGL expression in cortical and hippocampal samples (by diagnosis)

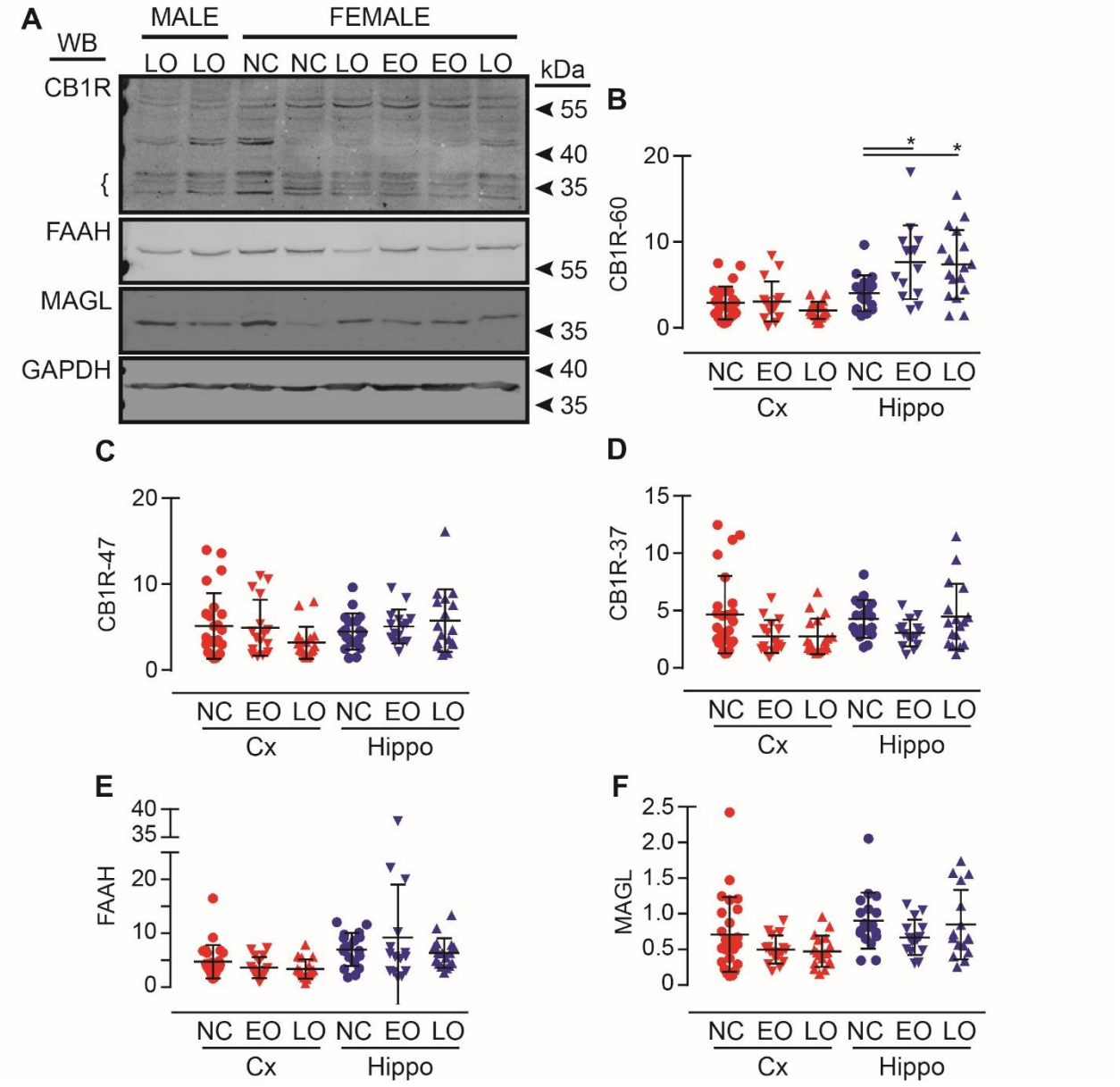

Figure 3: Alignment of cortical CB1R species by sex alone

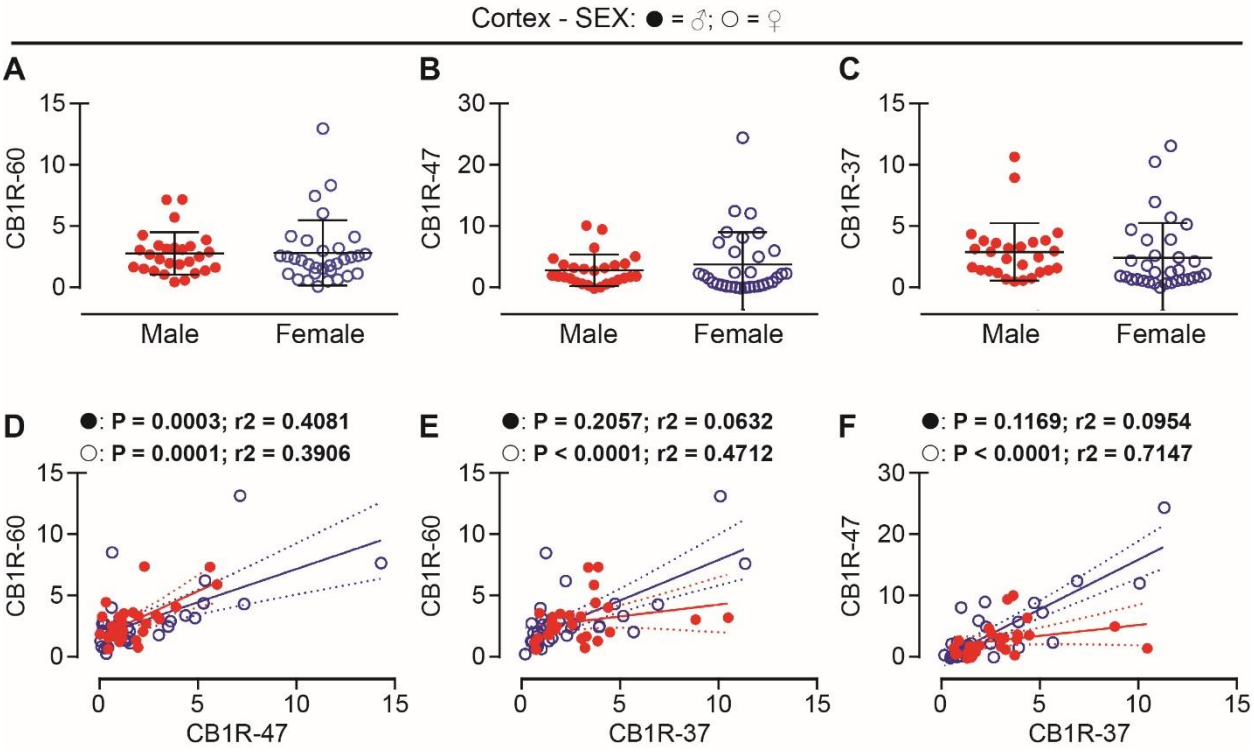

Figure 4: Alignment of FAAH and MAGL by sex alone

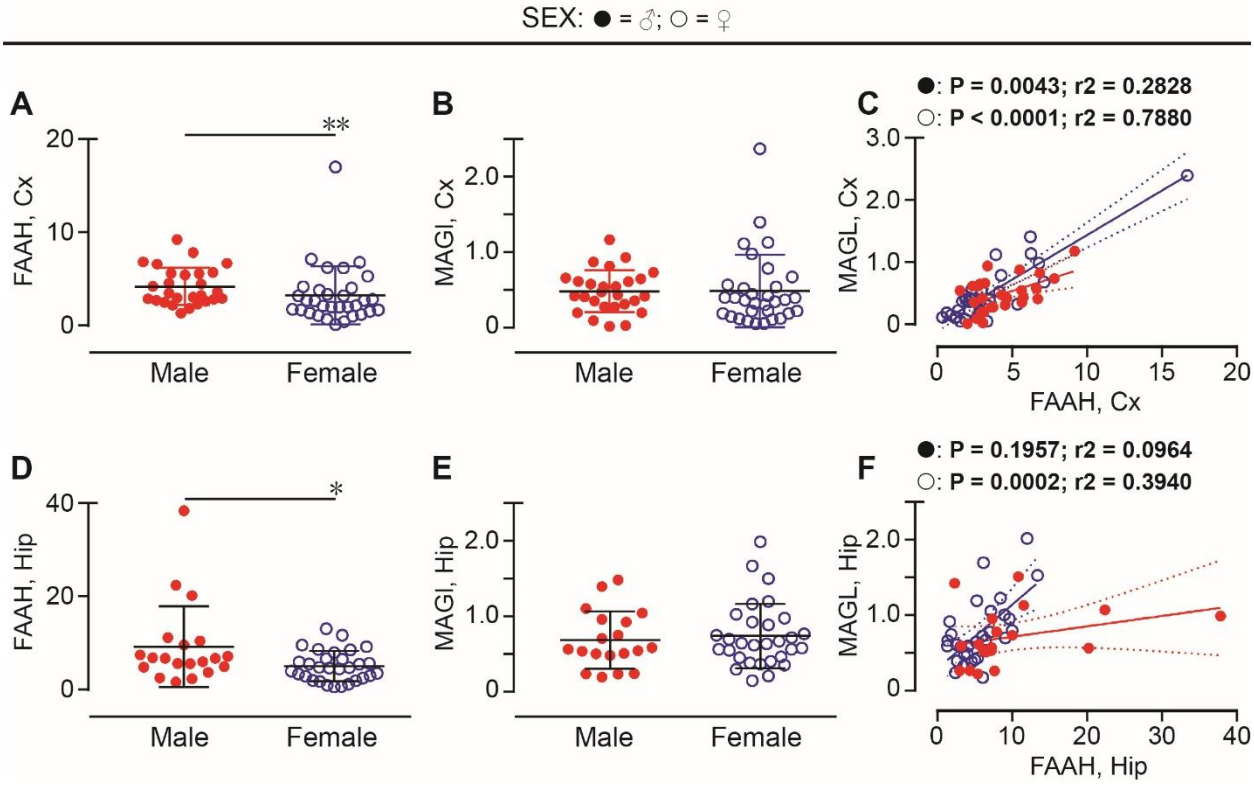

Figure 5: Alignment of cortical CB1R species with either FAAH or MAGL by sex alone

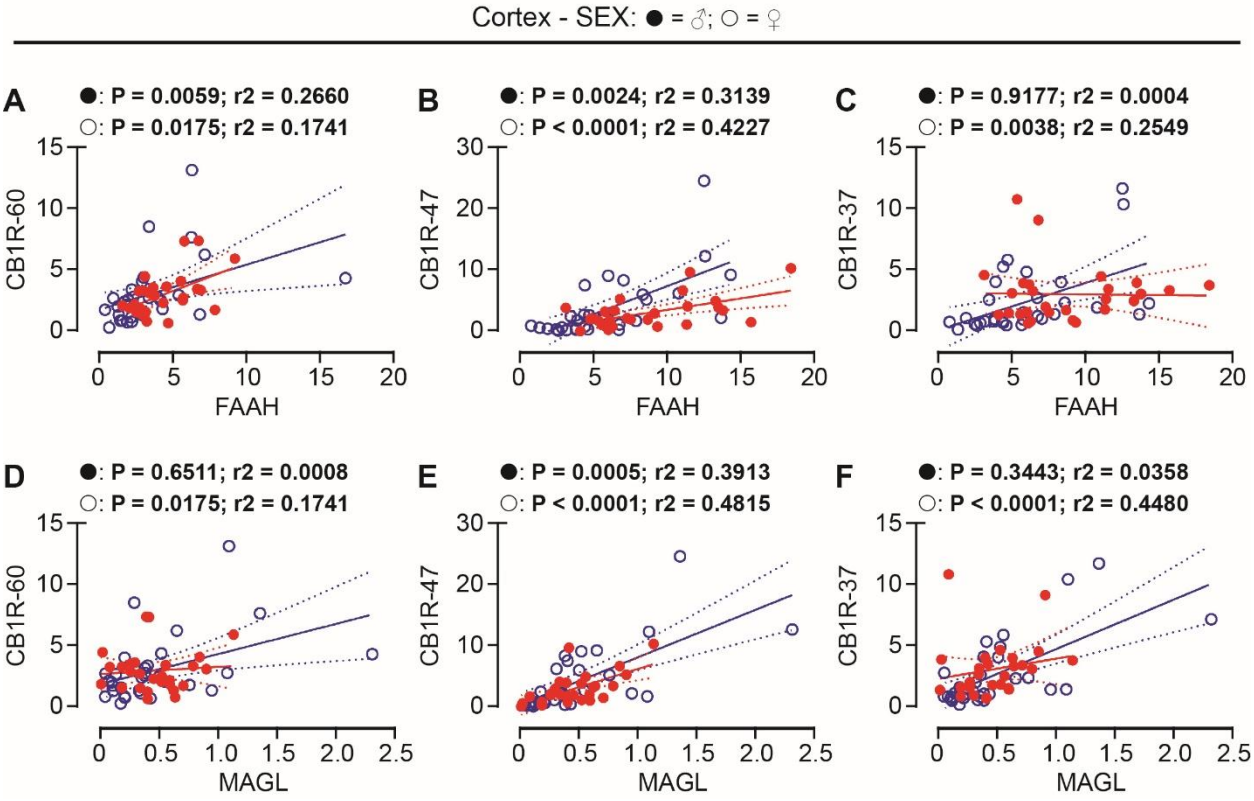

Figure 6: Alignment of FAAH and MAGL by diagnosis - cortex

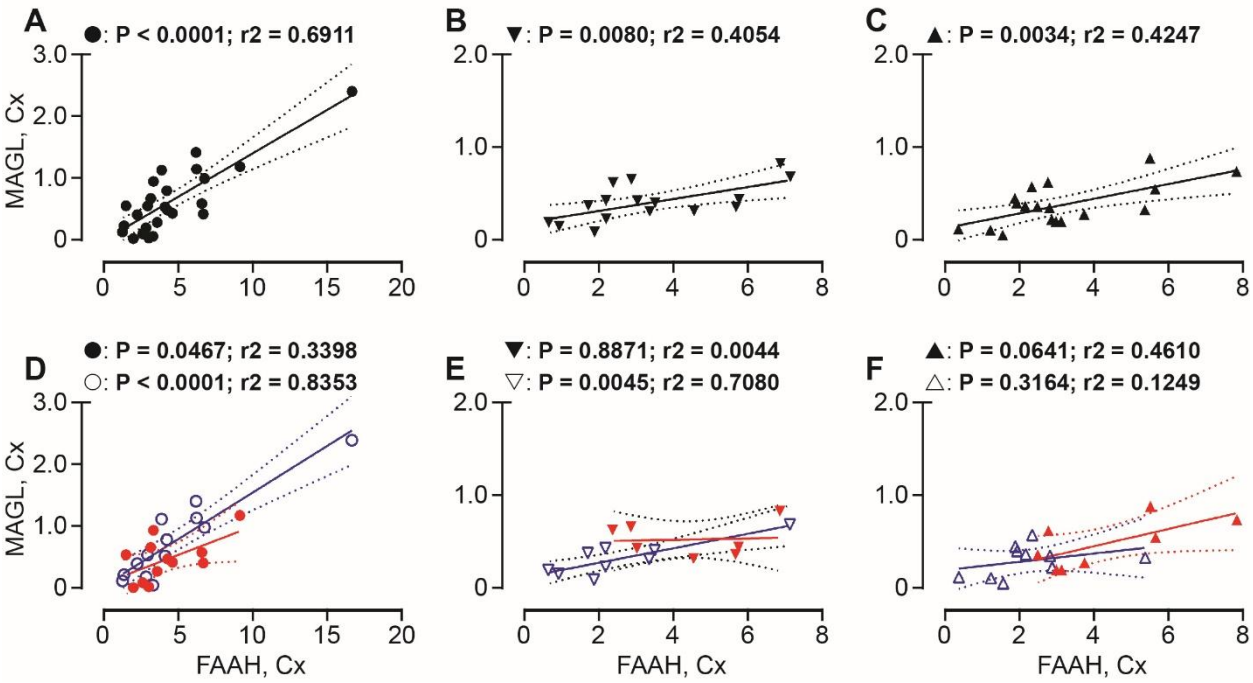

Figure 7: Alignment of FAAH and MAGL by diagnosis - Hippocampus

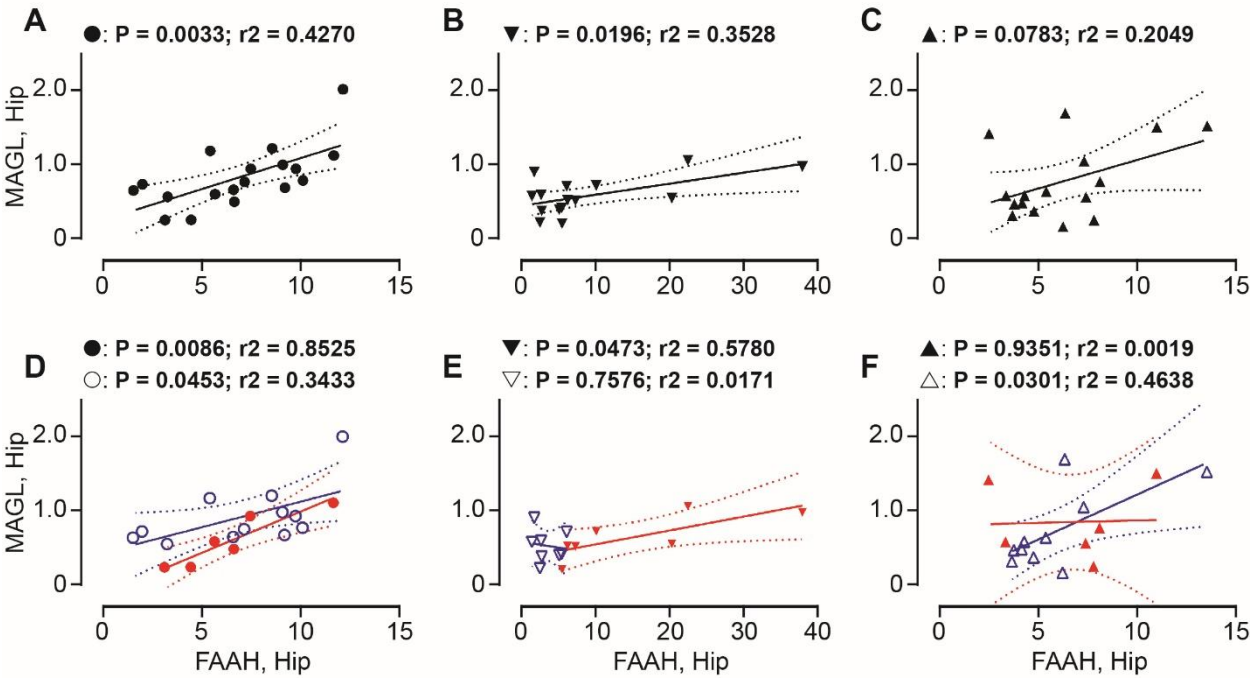

Figure 8: Alignment of CB1R species by MAGL by diagnosis - cortex

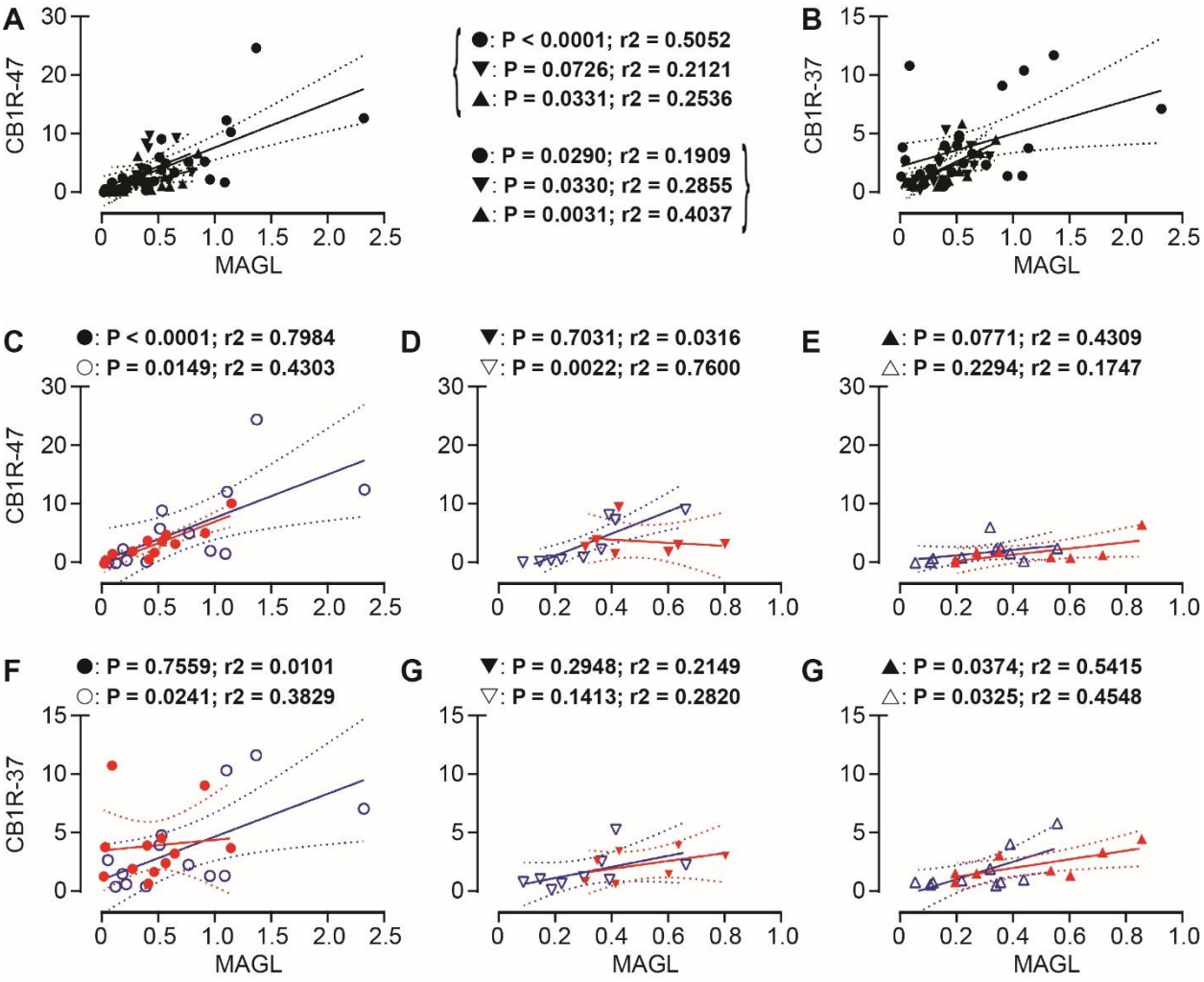

Figure 9: Alignment of CB1R species by APOE4 status - cortex

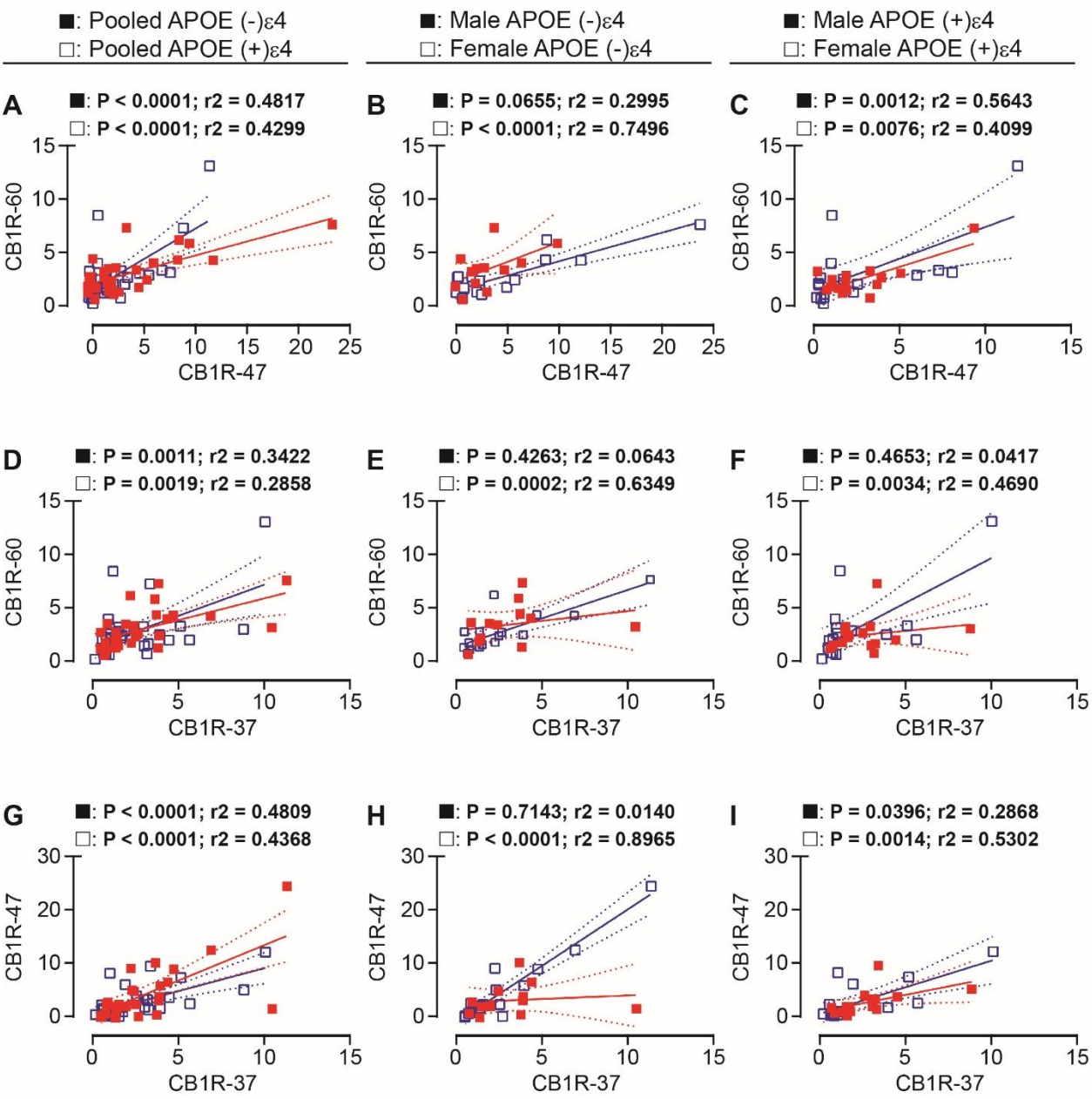

Figure 10: Alignment of FAAH and MAGL in Cx and Hippo by APOE4 status

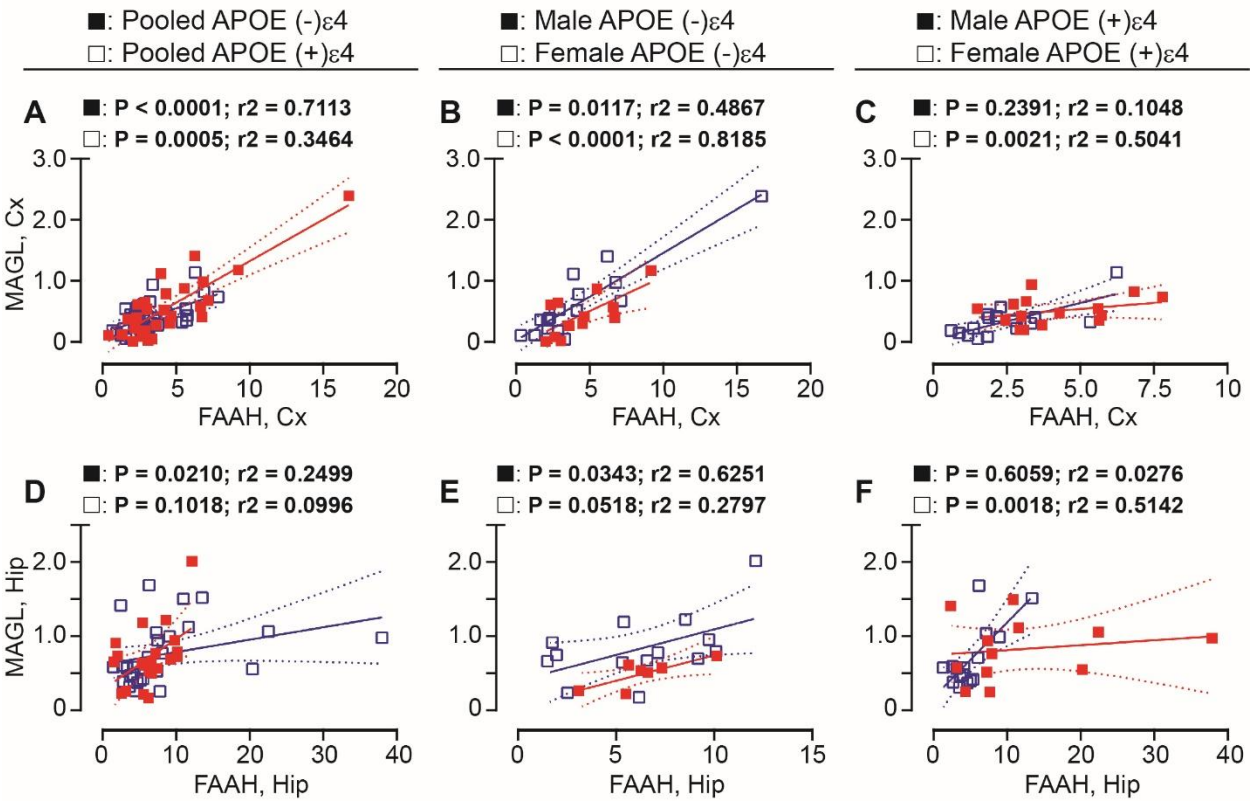

Figure 11: Alignment of cortical FAAH with CB1R species by APOE4 status

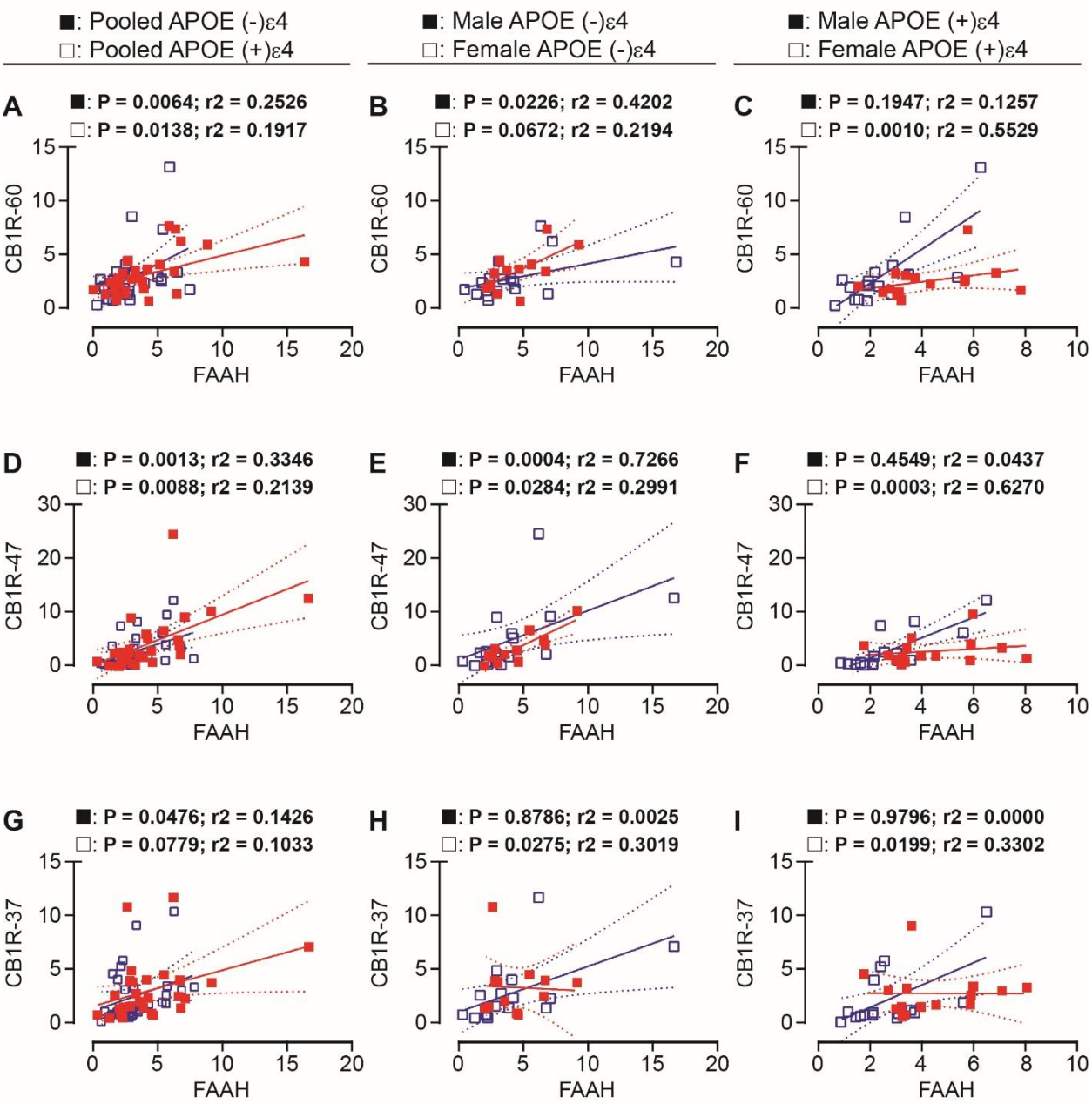

Figure 12: Alignment of cortical MAGL with CB1R species by APOE4 status

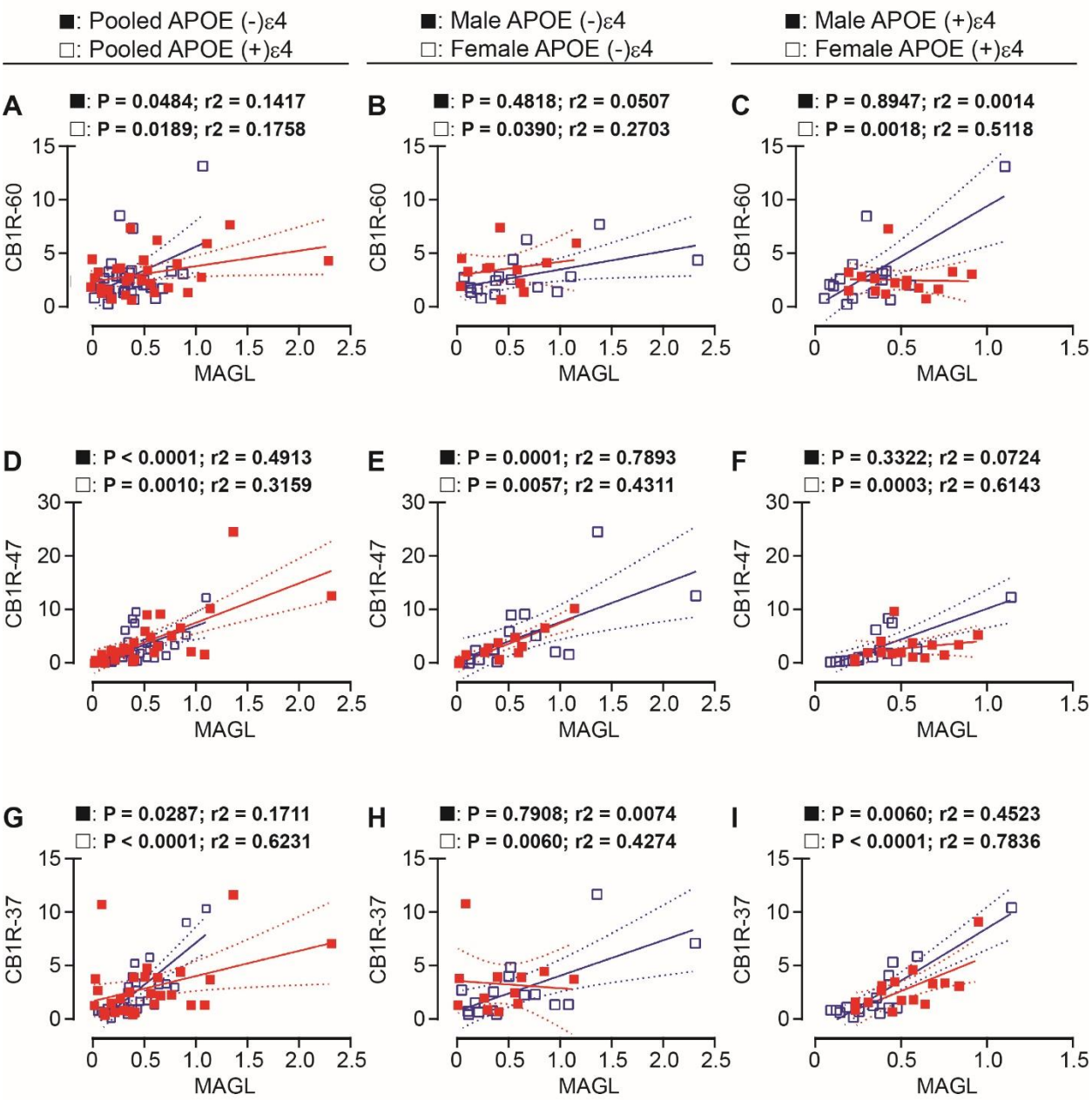

Supplementary Figures 1-4: These figures include information, primarily mean expression levels, in which only sporadic associations ($P < 0.05$) were observed.

Supplementary Figure 1. Expression levels of (**A**) CB1R-60, (**B**) CB1R-47, and (**C**) CB1R-37 in human cortical and hippocampal samples stratified by sex alone [●: male; ○: female].

Supplementary Figure 2. Expression levels of (**A**) CB1R-60, (**B**) CB1R-47, and (**C**) CB1R-37 in human cortical and hippocampal samples stratified by donor's *APOE* ε4 status [*e.g.* [■: (-)ε4; non-carriers; □: (+)ε4: carriers]. **: P <0.01 between indicated groups.

Supplementary Figure 3. Expression levels of CB1R-60, CB1R-47, and CB1R-37 in human cortical (**A-C**) and hippocampal (**D-F**) samples stratified by *APOE* ε4-by-sex [*e.g.* [■: male; □: female]. **: P <0.05 between indicated groups.

Supplementary Figure 4. Expression levels of FAAH and MAGL in human cortical (**A, B**) and hippocampal (**C, D**) samples stratified by *APOE* ε4-by-sex [*e.g.* [■: male; □: female].

Supplementary Tables 1-28: These tables include all of the regression analyses from this project.

Supplementary Files

This is a list of supplementary files associated with this preprint. Click to download.

- SuppTable128HeistadECSinADbrain2026.pdf
- SUPPLFig14HeistadECSinADbrainFINAL.pdf